JCI The Journal of Clinical Investigation

Targeting hepatic kisspeptin receptor ameliorates non-alcoholic fatty liver disease in a mouse model

Stephania Guzman, … , Andy V. Babwah, Moshmi Bhattacharya

J Clin Invest. 2022. https://doi.org/10.1172/JCI145889.

Research In-Press Preview **Hepatology** **Metabolism**

Graphical abstract

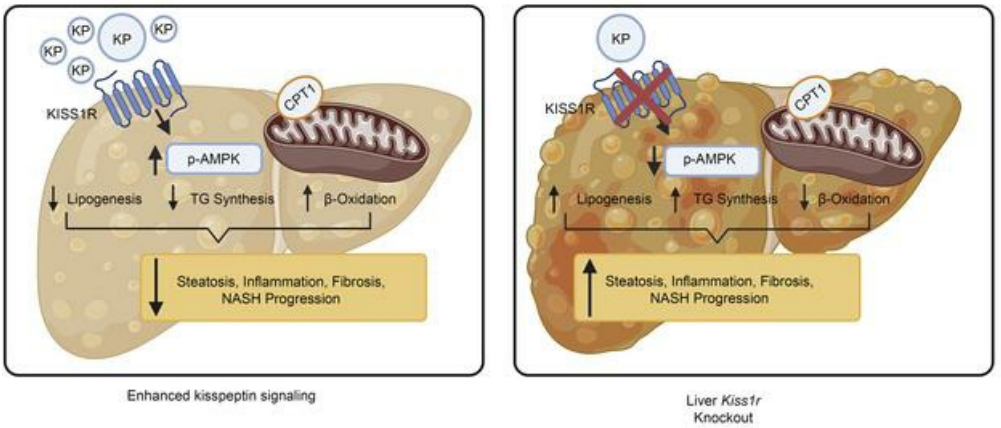

Targeting hepatic kisspeptin receptor ameliorates non-alcoholic fatty liver disease in a mouse model

Stephania Guzman[1,2], Magdalena Dragan[1], Hyokjoon Kwon[1], Vanessa de Oliveira[1], Shivani Rao[1], Vrushank Bhatt[3], Katarzyna M. Kalemba[1], Ankit Shah[1], Vinod K Rustgi[1], He Wang[4], Paul R. Bech[5], Ali Abbara[5], Chioma Izzi-Engbeaya[5], Pinelopi Manousou[6], Jessie Y. Guo[1,3], Grace L. Guo[7], Sally Radovick[8], Waljit S Dhillo[5], *Frederic E. Wondisford[1], *Andy V. Babwah[8,9], *Moshmi Bhattacharya[1,2,3,9]

[1]Department of Medicine, Robert Wood Johnson Medical School, Rutgers University; [2]Rutgers Center for Lipid Research, New Jersey Institute for Food, Nutrition, and Health, Rutgers University; [3]Rutgers Cancer Institute of New Jersey, New Brunswick, NJ; [4]Department of Pathology and Laboratory Medicine, Robert Wood Johnson Medical School, Rutgers University; [5]Section of Endocrinology & Investigative Medicine and [6]Department of Metabolism, Digestion and Reproduction, Imperial College London, United Kingdom; [7]Department of Pharmacology and Toxicology, School of Pharmacy, Rutgers University. [8]Department of Pediatrics, Robert Wood Johnson Medical School, Rutgers University; [9]Child Health Institute of New Jersey, New Brunswick, NJ, USA.

*** Co-senior authors**

Corresponding Author:

Dr. Moshmi Bhattacharya, Department of Medicine, Robert Wood Johnson Medical School, Rutgers University, Clinical Academic Building, Room 7148, 125 Paterson St., New Brunswick, NJ, 08901 USA, E-mail: mb1722@rutgers.edu Phone: 732-235-5269

Conflict of Interest

WSD / AA have provided consultancy services for Myovant Sciences Ltd. of no relevance to this work. M. Bhattacharya, A Babwah, F. Wondisford and S. Radovick are co-inventors on a provisional patent application (pending), filed by Rutgers University. All other authors have declared no conflict of interest.

Abstract

Nonalcoholic fatty liver disease (NAFLD), the most common liver disease has become a silent worldwide pandemic. The incidence of NAFLD correlates with the rise in obesity, type 2 diabetes and metabolic syndrome. A hallmark feature of NAFLD is excessive hepatic fat accumulation or steatosis, due to dysregulated hepatic fat metabolism which can progress to nonalcoholic steatohepatitis (NASH), fibrosis and cirrhosis. Currently, there are no approved pharmacotherapies to treat this disease. Here we have identified that activation of the kisspeptin receptor (KISS1R) signaling pathway has therapeutic effects in NAFLD. Using high fat diet-fed mice, we demonstrated that a deletion of hepatic *Kiss1r* exacerbated hepatic steatosis. In contrast, enhanced stimulation of KISS1R protected against steatosis in wild-type C57BL/6J mice and decreased fibrosis using a diet-induced mouse model of NASH. Mechanistically, we found that hepatic KISS1R signaling activates the master energy regulator, AMPK, to thereby decrease lipogenesis and progression to NASH. In NAFLD patients and in HFD-fed mice, hepatic KISS1/KISS1R expression and plasma kisspeptin levels were elevated, suggesting a compensatory mechanism to reduce triglyceride synthesis. These findings establish KISS1R as a therapeutic target to treat NASH.

Introduction

The liver is the principal organ involved in lipid metabolism. Dyslipidemia leads to metabolic disorders such as non-alcoholic fatty liver disease (NAFLD), which has become an increasing public health concern affecting approximately 25% of the population, globally (1). In the U.S., NAFLD is a national epidemic that affects about 85 million adults and 8 million children, with associated annual medical costs of $103 billion (2, 3). The prevalence of NAFLD mirrors the rise in obesity and type 2 diabetes (T2D). In both adult and pediatric disease, NAFLD is more common in males than females (4). NAFLD is characterized by accumulation of liver fat (steatosis or nonalcoholic fatty liver, NAFL) leading to the generation of cytotoxic lipid oxidation by-products along with other hepatic insults, which progresses to a chronic inflammatory state with hepatocyte injury, defined as non-alcoholic steatohepatitis (NASH). As the disease advances, a subset of patients will develop fibrosis, cirrhosis and liver failure or hepatocellular carcinoma (HCC) (5). NASH has replaced hepatitis C as the most common indication for liver transplantation (6). Currently, there are no approved pharmaceutical medicines for the treatment of NAFL/NASH.

Kisspeptins (KPs), the peptide products of the *KISS1* gene, are endogenous ligands for the kisspeptin 1 receptor (KISS1R), a $G\alpha_{q/11}$ protein-coupled receptor. The KP/KISS1R signaling system is expressed both centrally in the brain and in peripheral organs, where it plays a major role in reproduction and metabolism (7, 8). In fact, liver *Kiss1* expression was found to be increased in genetic models of obesity (db/db and ob/ob mice) (9). Although *KISS1* and *KISS1R* are expressed in the liver (10), a role for hepatic KISS1R signaling in lipogenesis is not known. In this study, using a high fat diet (HFD)-induced mouse model of NAFLD, we demonstrate that a hepatic knock-out of *Kiss1r* exhibits liver steatosis. In contrast, activation of hepatic KISS1R using a potent kisspeptin agonist (KPA) protects against the development of hepatic steatosis and found

to reduce progression to NASH and hepatic fibrosis. Mechanistically, it was observed that hepatic KP signaling activates AMPK to thereby exert its protective effects. HFD induced the expression of hepatic *Kiss1* and *Kiss1r* and increased plasma KP levels in mouse models; these observations were recapitulated using clinical samples. This study provides direct evidence that both pharmacological and genetic interventions directed at KISS1R-mediated signaling pathway can protect against the development of NAFLD.

Results

Hepatic KISS1R deficiency aggravates hepatic steatosis in insulin resistant obese mice

To test whether hepatic KISS1 and KISS1R are involved in the pathogenesis of NAFLD, hepatic *Kiss1* and *Kiss1r* expression was measured in a HFD-induced mouse model of NAFLD. Here, it was observed that after wild-type male C57BL/6J mice were fed a HFD for 12 weeks, hepatic *Kiss1* and *Kiss1r* mRNA expression significantly increased compared to mice maintained on regular diet (RD) (**Figure 1A**). In contrast, no change was observed in *Kiss1r* and *Kiss1* mRNA expression in other tissues upon administration of HFD (**Supplemental Figures 1A, 1B)**. KPs are secreted peptides and the liver is a major source of KPs (9). Plasma KP levels were measured in C57BL/6J mice on either RD or HFD. HFD-fed mice had significantly increased circulating KP levels compared to mice on RD (**Figure 1B**). Next, to investigate a role for KISS1R in regulating hepatic lipid metabolism, a mouse liver-specific knockout of *Kiss1r* (LKO) was generated. Analysis of the LKO mice showed that *Kiss1r* expression, but not *Kiss1,* was significantly reduced in the liver (**Supplemental Figures 1C, D**). *Kiss1r* expression was unaffected in other metabolic organs under HFD conditions (**Supplemental Figure 1C**).

HFD of 20 weeks duration but not RD, induced steatosis in LKO mice (**Figures 1C, 1D**) and resulted in an increase in liver triglycerides (TG), compared to controls (**Figure 1E**). Serum alanine transaminase (ALT) levels were significantly elevated in HFD-fed LKO group compared to HFD-fed controls, suggesting enhanced HFD-induced hepatocellular injury in LKO mice (**Figure 1F**). Importantly, this phenotype is not due to differences in testosterone levels in HFD-fed LKO mice and controls since these were not significantly different (**Supplemental Figures 1E**). As previously reported (11), there was a decrease in testosterone levels in HFD groups, although not significant in our studies (**Supplemental Figures 1E**). Since hyperglucagonemia has been observed in NAFLD (12), we measured plasma glucagon levels and observed a non-significant increase in HFD-fed LKO mice (**Supplemental Figures 1F).** LKO mice also exhibited an increase in inguinal white adipose tissue compared to controls on HFD, although no differences were observed in epididymal white adipose tissue between groups (**Supplemental Figures 1G, H**, respectively). HFD-fed LKO mice displayed significantly increased body weights compared to controls (**Supplemental Figure 2A**), and significantly reduced energy expenditure (**Supplemental Figure 2C**), despite showing no differences in food intake (**Supplemental Figure 2B**) or ambulatory activity (**Supplemental Figures 2D**). Respiratory ratio (RER) was significantly increased in LKO HFD groups during the light phase (i.e resting phase of the nocturnal animals); this suggests that LKO mice on HFD have a decrease in the use of endogenous lipids as fuel source and/or increased rate of de novo lipogenesis **(Supplemental Figures 2E).** Taken together, the increase in liver TGs in the LKO HFD mice suggests that hepatic KISS1R plays a protective function against steatosis.

Hepatic KISS1R deficiency upregulates the expression of genes involved in lipogenesis

To elucidate the mechanism underlying hepatic lipid accumulation in LKO mice, the mRNA levels of hepatic regulators of fatty acid uptake [the fatty acid translocase (*Cd36*) and liver fatty acid-binding protein, (*Lfabp1*)], as well as lipogenesis [sterol regulatory element binding protein-1c (*Srebp1c*), fatty acid synthase (FAS, encoded by *Fasn*) and acetyl-CoA carboxylase 1 (ACC1, encoded by *Acaca*) which catalyzes the first committed step of *de novo* fatty acid synthesis were measured. It was observed that under HFD conditions, livers from LKO mice showed a significant upregulation of the expression of all genes (**Figure 2A**) including peroxisome proliferator-activated receptor γ (PPARγ, encoded by *Pparg*), a key regulator of lipogenesis that is induced in steatotic livers of NAFLD patients and experimental models (13, 14).

PPARγ2, in contrast to PPARγ1 is induced upon HFD feeding and is linked to the development of NAFLD (15). Protein levels of PPARγ2 (**Figure 2B**, top band in immunoblot), and its downstream gene targets CD36 and FAS were significantly higher in the HFD LKO livers compared to controls (**Figure 2B, Supplemental Figures 3A-C**). PPARγ2 is negatively regulated by mitogen-activated protein kinases (MAPK)-dependent phosphorylation at Ser-112 (16). A decrease in PPARγ2 phosphorylation at this inhibitory site was observed in LKO livers (**Figure 2B, Supplemental Figure 3D**). Additionally, LKO livers exhibited suppressed phosphorylation of endogenous AMPK on the α-subunit at Thr-172, a crucial phosphorylation site in the activation of AMPK (17) (**Figure 2B, Supplemental Figure 3E**). AMPK is a protein kinase that when activated inhibits *de novo* lipogenesis (DNL), by negatively regulating SREBP1 activity and its downstream gene targets such as *Acaca* and *Fasn (18)*. These data suggest that hepatic KISS1R deficiency in HFD-fed LKO mice increases lipogenesis in liver.

Hepatic KISS1R deficiency modulates genes involved in TG synthesis and mitochondrial function

Triglyceride (TG) synthesis (**Figure 2C**) requires glycerol 3-phosphate, which can be formed by glycerol kinase (GK)-dependent phosphorylation of glycerol. An analysis of the livers from the HFD LKO mice revealed a significant increase in the hepatic expression of GK, (a PPARγ gene target) compared with HFD control mice (**Figures 2B, D, Supplemental Figure 3F**). Previous studies have also demonstrated that HFD induces GK expression (19). Glycerol enters the liver primarily via aquaglyceroporins (AQP) such as AQP3 and AQP9 (**Figure 2C**) (20, 21). *Aqp9* mRNA levels were significantly upregulated in LKO HFD mice livers, whereas *Aqp3* levels remained unchanged (**Figure 2D**). Many enzymes regulating TG synthesis, including glycerol-3-phosphate acyltransferase (GPAT1, encoded by *Gpam*) that catalyzes the rate limiting step in TG synthesis, diacylglycerol acyltransferase 2 (*Dgat2*, acylates diacylglycerol to form TG), and monoacylglycerol acyltransferase 1 (*Mogat1*, coverts monoacylglycerol to diacylglycerol the direct precursor of TG) (**Figure 2C**), were also upregulated in LKO HFD livers (**Figures 2B, D; Supplemental Figure 3G-I**). MOGAT expression is also regulated by PPARγ (15). In contrast, no changes were seen in the expression of key regulators of lipogenesis or TG synthesis in the livers of LKO mice maintained on RD (**Supplemental Figures 2F-N).** Taken together, this demonstrates that hepatic knockout of *Kiss1r* in HFD mice results in an upregulation of genes regulating TG synthesis.

LKO HFD mice livers displayed decreased levels of mitochondrial carnitine palmitoyltransferase 1 α (CPT1α), a regulatory enzyme that transfers fatty acids from the cytosol to mitochondria prior to β-oxidation (**Figure 2E**). This data suggest that hepatic steatosis develops in LKO mice as a result of increased lipogenesis (**Figure 2 A-D**) and impaired fatty acid oxidation. In NAFLD, when cytosolic fatty acids accumulate due to impaired β-oxidation, alternative

pathways in microsomes (ω-oxidation) are activated in a compensatory capacity. This was observed in LKO HFD livers that exhibited elevated levels of CYP4As (*Cyp4a10, Cyp4a14*) that catalyze ω-oxidation (**Figure 2E**). Collectively, these data suggest that hepatic steatosis develops in LKO mice due to increased DNL and TG synthesis and impaired mitochondrial β-oxidation.

Hepatic KISS1R deficiency alters lipidomic profiling in liver extracts

To identify metabolic differences contributing to the distinct phenotypes observed in LKO mice under HFD conditions, a global untargeted metabolomic analysis of LKO (LKO HFD) and control (CTRL HFD) livers was conducted. This revealed that various lipids including TG, DAG, and lysophosphatidylcholine were significantly upregulated in HFD LKO livers (**Figure 2F**). Similar observations were also seen in patients with NAFLD and NASH (22). Livers from LKO HFD mice also exhibited other changes, including high levels of ceramides, phosphatidylglycerol and cardiolipin. The inhibition of ceramide synthesis was reported to attenuate hepatic steatosis and fibrosis while phosphatidylglycerol, a mitochondrial phospholipid, is implicated in multiple metabolic diseases including hepatosteatosis (22). Cardiolipin is a phospholipid that is essential for optimal mitochondrial function and alterations contribute to mitochondrial dysfunction in multiple tissues including insulin resistance and NAFLD (23).

Hepatic KISS1R deficiency promotes insulin resistance, hepatic inflammation and hepatic fibrosis biomarkers

Since selective insulin resistance plays an important role in the pathogenesis of NAFLD, metabolic tests were performed to examine the effect of the loss of hepatic KISS1R on glucose homeostasis. Compared to HFD-fed controls, LKO HFD mice had significantly higher fasting

glucose levels, indicative of elevated gluconeogenesis (**Figure 3A**). They were also glucose intolerant (**Figures 3B, C**) and insulin resistant (**Figures 3D, E**). Consistent with the insulin resistance phenotype, basal insulin levels were significantly upregulated in the LKO mice on HFD, compared to the controls on the same diet (**Figure 3F**).

NAFL can progress to NASH, a state associated with increased inflammation, fibrosis and oxidative stress in the liver (24). HFD-feeding induces insulin resistance, liver steatosis and modest inflammation but does not cause significant hepatocyte injury or fibrosis (25, 26). We observed that there was an upregulation of various markers involved in inflammation and early stages of fibrosis in LKO mice after 20 weeks of HFD. These included inflammatory markers associated with NASH (27-29) such as macrophage inflammatory protein 2 (*Mip2),* chemokines interferon gamma-induced protein 10 *(Ip10),* interleukin-1α (*Il1a*), and proinflammatory cytokine tumor necrosis factor (TNF)-α (*Tnfa*) (**Figure 3G**). Serum levels of interleukin-1α (IL-1α) were elevated in LKO mice on HFD compared to controls (**Figure 3H)**. Various markers of fibrosis such as collagen (*Col1a2*), smooth muscle actin (*Acta2*), matrix metalloproteinases (*Mmp2, Mmp13*) and transforming growth factor β (*Tgfb*) were upregulated in the livers of LKO (HFD) group (**Figure 3I),** although at the protein level only smooth muscle actin (SMA) was significantly different **(Figure 3J, Supplemental Figure 3J-M**). This is not surprising given that HFD feeding alone induces modest inflammation (25, 26) and does not cause substantial hepatocyte injury or fibrosis(30). Together, these findings suggest that loss of hepatic KISS1R signaling exerts a deleterious effect on the liver, by increasing hepatic steatosis and the progression to NASH.

KISS1R agonist alleviates hepatic steatosis and metabolic deterioration in a wild-type mouse model of NAFLD

Next, we determined the effect of enhanced KISS1R signaling on the development of NAFLD. Wild-type C57BL/6J mice (5-6 weeks of age) were placed on either RD or HFD for 6 weeks. Mice on HFD gained weight **(Supplemental Figure 4A)** and developed insulin resistance, resulting in elevated fasting glucose levels (**Supplemental Figure 4B**). Mice (littermates, with similar body weights) were then infused with vehicle (PBS) or a KP-analog, TAK-448 (0.3 nmol/hr, henceforth referred to as KPA). This dose is based on published studies using KP in animal models and adjusted based on weight (31, 32). This synthetic KP-analog potently stimulates KISS1R activity in animal and human (33-36). Mice were maintained on RD or HFD for another 5 weeks. KPA-treated HFD-fed mice had significantly lower fasting glucose levels compared to VEH group controls (**Figure 4A**). Consistent with these phenotypes, HFD KPA-treated mice were glucose tolerant (**Figures 4B, Supplemental Figure 4C**), insulin sensitive (**Figures 4C, Supplemental Figure 4D**) with significantly lower basal insulin (**Figure 4D**) and glucagon levels (**Supplemental Figure 4E)**, compared to HFD VEH-treated controls.

In addition to the effects of KPA treatment on improved glucose homeostasis, KPA treatment had a striking protective effect against the development of steatosis in the HFD-fed mice (**Figure 4E**), resulting in a significant decrease in liver TGs (**Figure 4F**). TGs are formed by esterification of FFA and glycerol and stored in hepatocytes. We found that serum levels of TGs, FFA and glycerol as well as cholesterol were significantly lower in the KPA-treated group on HFD (**Figures 4G-J**). Importantly, KPA treatment significantly reduced serum ALT levels (**Figure 4K**), which indicated less liver injury. Among the HFD mice, KPA-treated mice had a slightly lower body weight than VEH controls (**Supplemental Figure 4F**), without change in food intake

(**Supplemental Figure 4G**). KP signaling is a key regulator of the hypothalamic–pituitary–gonadal axis (HPG) (37). Importantly, prolonged exposure to KPA did not significantly affect the HPG axis, based on testosterone levels (**Supplemental Figure 4H**). KPA-treated mice showed significantly increased energy expenditure in the light phase and had lower RER in light and dark phase, suggesting that fat metabolism is enhanced in KPA-treated mice (**Supplemental Figure 4I, J**) without significant changes in movement (**Supplemental Figure 4K)**. Additionally, KPA-treated mice had significantly lower white epididymal and inguinal adipose tissue (**Supplemental Figures 4L, M**).

Mechanistically, KPA treatment under HFD conditions significantly reduced the hepatic expression of key regulators of TG synthesis such as PPARγ and its target genes, CD36 and MOGAT1 (**Figures 4L, 5A, Supplemental Figures 5A-C**). PPARγ2 activity is negatively regulated by MAPK-dependent phosphorylation at Ser-112 (16, 38, 39). It is established that KISS1R signaling activates MAPK (7, 40). KPA treatment stimulated phosphorylation of PPARγ2 at Ser-112, suggesting that a possible mechanism by which KISS1R regulates PPARγ2 is via MAPK (**Figure 5A, Supplemental Figure 5D**). Furthermore, KPA treatment induced phosphorylation of AMPK at Thr-172 (**Figure 5A, Supplemental Figure 5E**), which inhibits PPARγ activity and transcription (41, 42). AMPK activation also inhibits lipid synthesis by the acute inhibition of GPAT1 activity and by negatively regulating SREBP1 transcription (43). GPAT mRNA and protein levels were significantly reduced in KPA-treated livers (**Figures 4L, 5A**; **Supplemental Figure 5F**), which could lead to the subsequent decrease in GPAT1 activity. We also observed a decrease in DGAT1 protein expression, although it was not significant (**Figure 5A**, **Supplemental Figure 5G).** It is noted that although the reduction in *Srebp1c* was not significant, there was a significant decrease in its downstream target, *Fasn* (**Figure 4L, 5A;**

Supplemental Figure 5H). KPA treatment also reduced the expression of *Lfabp1* and *Gk1* (**Figures 4L, 5A**, **Supplemental Figure 5I, J**). However, KPA treatment increased expression of *Cpt1a* and *Cpt2*, rate-limiting enzymes for mitochondrial fatty acid transportation and also increased the expression of acyl-coenzyme A oxidase (*AOX*), which regulates the rate-limiting step of peroxisomal β-oxidation of fatty acids (**Figure 5B**). Since hepatic lipolytic enzymes adipose triglyceride lipase (ATGL) and hormone sensitive lipase (HSL) regulate hepatic TG metabolism by increasing lipolysis and promoting fatty acid oxidation (44), we examined whether KPA regulated the phosphorylation status of these enzymes. A significant increase in phosphorylation of both enzymes was observed in livers from KPA-treated mice, which suggests increased activity and lipolysis (**Figure 5C**). Thus, KPA administration in vivo appears to enhance hepatic lipolysis and mitochondrial and peroxisomal β-oxidation.

Livers from KPA-mice had suppressed levels of genes regulating pro-inflammatory markers (*Ip10, Mcp1, Il1a*) (**Figure 5D**). Serum levels of IL−1α were lower in KPA-treated groups (**Figure 5E**), although significance was not reached. Interleukin 1β (IL−1β) plays a major role in the progression of steatosis to steatohepatitis and liver fibrosis (45) and levels were decreased at mRNA and protein levels, although not significantly (**Figure 5D, G; Supplemental Figure 5K)**. Decreases in various markers for fibrosis were observed in KPA-treated livers (**Figure 5F, G, Supplemental Figure 5L-N**); however, HFD feeding alone did not strongly induce inflammation or establish fibrosis. In contrast, no significant differences in the expression of key regulators of lipogenesis or TG synthesis were observed in age-matched C57BL/6J mice maintained on RD, upon KPA treatment (**Supplemental Figure 6).** This is consistent with the lack of increase in liver TGs observed in KPA treated mice, compared to controls maintained on RD (**Figure 4F**). Only glycerol kinase protein levels were significantly lower in KPA-treated groups (**Supplemental**

Figure 6C, F), but no change in mRNA was observed (**Supplemental Figure 6B).** No differences were observed between control and KPA-treated groups for the regulation of glucose homeostasis under RD conditions (**Figure 4B, C).** Next, to understand the specific role of hepatic *Kiss1* in NAFLD, we depleted *Kiss1* levels (**Supplemental Figure 7A)** by expressing AAV8-U6-mKISS1-shRNA (shKiss1) or scrambled (SCRM) controls. Surprisingly, in male mice on HFD, depletion of hepatic *Kiss1* had no effect on steatosis, liver TGs and the expression of key regulators of lipogenesis, triglyceride synthesis and inflammation **(Supplemental Figure 7A-F).** Additionally, no differences in body weight or glucose homeostasis were noted (**Supplemental Figure 7G-J).** Taken together, this suggests that kisspeptin critically exerts its protective effect in vivo under pathophysiological conditions by activating hepatic KISS1R to downregulate lipid synthesis via AMPK activation, as well as increasing β-oxidation, thus attenuating the development of NAFLD.

KISS1R agonist fails to protect against steatosis and NASH progression in a hepatic Kiss1r deficient mouse model

Data show that activation of KISS1R by KPA had a beneficial effect, significantly reducing hepatic steatosis and decreasing NASH progression in mice fed HFD (**Figures 4, 5**). In order to verify that liver-specific KISS1R signaling was crucial to mediate the protective effects of KPA, we investigated the effect of KPA on LKO mice placed on HFD for 6 weeks prior to administration of vehicle (VEH) or KPA for 5 weeks on HFD. The protective effect of KPA on steatosis was lost (**Figure 6A**), and levels of liver and serum TGs (**Figure 6B, C**), serum ALT, FFA and cholesterol (**Figure 6D-F**) were similar between VEH and KPA-treated LKO mice. No differences were observed between the two groups for body weight, glucose homeostasis or adiposity (**Supplemental Figure 8A-E).** Furthermore, there were no significant differences in the

expression of key regulators of lipogenesis, TG synthesis, inflammatory and fibrosis markers (**Figure 6G-J, Supplemental Figure 8F-N)**. This provided 'on-target' confirmation that the protective effect on steatosis and NASH progression is due to direct hepatic *Kiss1r* signaling by regulating these key metabolic pathways.

KISS1R agonist fails to protect against steatosis and NASH progression in hepatic AMPK depleted mice.

To dissect the in vivo contribution of hepatic AMPK in mediating the protective effects of kisspeptin signaling in NAFLD, the expression of AMPKα2 was depleted in the livers of C57BL/6J mice on HFD (**Figure 7A, B, Supplemental Figure 9A, B**). This isoform has been shown to critically control hepatic lipogenesis (46). Mice were placed on HFD for 4 weeks then injected with either AAV8-U6-M-PRKAA2-shRNA (shAMPK) or scrambled controls (SCRM). Mice were maintained on HFD for another 3 weeks before KPA was administered to SCRM and shAMPK groups for 6 weeks on HFD. There were no significant changes observed in body weight (**Supplemental Figure 9C**) or energy expenditure, RER or movement (data not shown) between the two groups. However, in contrast to KPA-treated controls, there was a marked increase in steatosis and Oil red O staining in the livers from the KPA-treated shAMPK mice (**Figure 7C**). Liver TGs, serum TGs and ALT levels were significantly elevated in shAMPK group (**Figure 7 D-F**). Various markers for lipogenesis and TG synthesis were upregulated in the shAMPK cohort (**Figure 7 G-I, Supplemental Figure 9D-J, Supplemental Figure 10**). Several inflammatory genes such as *Mip2, Ip10, Il1a* (**Figure 7J**), and serum levels of TNFα (**Figure 7K**) and IL1-β protein levels (**Figure 7M, Supplemental Figure 9K, Supplemental Figure 10C**) were increased in the KPA-treated shAMPK group. Markers for fibrosis such as MMP2, MMP9 and

MMP13 and smooth muscle actin were markedly elevated in KPA-treated shAMPK mice (**Figure 7L, M**, **Supplemental Figure 9 L-O**). However, significant differences were not observed in *Col1a1* mRNA levels (**Figure 7L**) and collagen 1 protein was undetected by Western blot analysis (data not shown). This is not surprising since 13 weeks of HFD is not sufficient to fully establish fibrosis (30). Levels of plasma ketone bodies serve as a surrogate marker for hepatic β-oxidation, and liver-specific AMPKα2 deletion decreases plasma ketone levels (46). KPA-treated shAMPK mice displayed a decrease in plasma ketone levels, compared to KPA-treated controls (**Figure 7N)**. Taken together, these data demonstrates that AMPK plays an essential role in mediating the protective effect of KPA in steatosis and in reducing the progression to NASH.

KISS1R agonist alleviates NASH in a Diet Induced Animal Model of Non-Alcoholic Liver Disease (DIAMOND) mice.

DIAMOND mice given a high fat 'Western' diet and sugar water (WDSW) develop obesity, insulin resistance, dyslipidemia and NAFL, which progresses to NASH and bridging fibrosis, closely resembling human NASH histologically (47). Next, to determine the impact of enhanced KISS1R signaling on advanced disease, KPA or vehicle was administered for 6 weeks to DIAMOND mice (fed WDSW for 33 weeks), while maintaining the same dietary regimen. WDSW for this duration in DIAMOND mice results in advanced NASH with bridging fibrosis (47). A significant decrease in liver weight and serum ALT levels was observed in KPA-treated mice (**Figure 8A, B**). As expected, DIAMOND mice livers showed signs of fibrosis based on picrosirius red staining **(Figure 8C**), an indicator of collagen deposition and hepatic injury resulting in scarring (48). KPA administration significantly decreased picrosirius red staining (**Figure 8C**), and also reduced the liver hydroxyproline levels (**Figure 8D**), which indicates true

collagen content (49). KPA treatment lowered the inflammatory markers (*Mip2, Il1a*), and there was a trend towards decreased serum IL-1α levels in KPA-treated mice (**Figure 8E, F**). Protein level of proinflammatory cytokine IL-1β was also significantly reduced in KPA-treated group (**Figure 8G, Supplemental Figure 11A**).

Prominent reduction in several fibrogenic genes and proteins was seen in KPA-treated DIAMOND mice including smooth muscle actin, MMPs, collagens and TGFβ, a critical mediator of hepatic fibrosis (**Figure 8G and H, Supplemental Figure 11B-G**). Significant decreases in liver TGs and hepatic Oil red O staining (that marks lipids) were noted in KPA-treated DIAMOND mice (**Figure 9A, B**), whereas there was a trend towards decrease in serum TGs (**Figure 9C**). The levels of serum FFA and cholesterol were significantly reduced in the KPA-treated group (**Figure 9D, E**). However, significant changes in expression of genes regulating lipogenesis were not observed except for *Mogat1* (**Figure 9F**), although a significant reduction in MOGAT protein was not detected (**Figure 9G, Supplemental Figure 11H).** Protein levels of DGAT and GPAT1 protein levels were decreased in KPA-treated mice (**Figures 9G, Supplemental Figure 11I, J**), although no changes between the two groups were observed in levels of GK or FAS (**Figures 9G, Supplemental Figure 11 K, L)**.

KPA-treated DIAMOND mice had slightly lower body weight, with no change in food intake (**Supplemental Figure 12 A, B),** and displayed significantly less adipose tissue **(Supplemental Figure 12 C, D).** These KPA-treated DIAMOND mice exhibited an increase in energy expenditure and decreased in RER in the light phase (resting period) (**Supplemental Figure 12 E, F)**; similar to what was observed with KPA-treated C57BL/6J wild-type mice **Supplemental Figure 4 I, J)**. Energy expenditure is regulated through the activity of uncoupling proteins (UCP) (50), and expression of UCP1 and UCP2 in brown adipose tissue (BAT) are

influenced by high fat diet (51). In particular, UCP2 oxidation has been shown to regulate BAT thermogenesis by favoring the utilization of free fatty acids (52). Interestingly, a significant increase in *Ucp2* mRNA expression was seen in BAT isolated from KPA-treated C57BL/6J mice on HFD, whereas BAT from DIAMOND mice on WDSW displayed increases in both *Ucp1* and *Ucp2* levels (**Supplemental Figure 12G, H)**. Peroxisome proliferator-activated receptor gamma coactivator 1 (PGC1α) strongly induces UCP in BAT (53). We observed significant increases in *Pgc1a* expression in both KPA-treated models **(Supplemental Figure 12G, H).** This suggests KPA promotes brown adipocyte mediated thermogenesis.

Similar to observations with C57BL/6J mice on HFD (**Figure 5A**), KPA induced AMPK phosphorylation in DIAMOND mice livers (**Figures 9H; Supplemental Figure 11M).** Increased AMPK phosphorylation and activity increase hepatic β-oxidation (54), which can be evaluated by measuring ketone levels. KPA-treated DIAMOND mice showed a trend towards increased levels of plasma ketone bodies (**Figure 9I**). KPA treatment significantly increased expression of *Cpt2* and *AOX*, key regulators of mitochondrial and peroxisomal β-oxidation of fatty acid, respectively in addition to increasing the levels of *Cyp4a10* and *Cyp4a14* that catalyze ω-oxidation of fat (**Figure 9J**). This is likely a potential mechanism by which hepatic lipid content decreases upon KPA administration.

It is established that AMPK signaling enhances energy metabolism, but it also represses inflammatory responses and inhibits NASH progression by suppressing liver NFκB (55). We therefore investigated whether KPA treatment regulates hepatic NFκB phosphorylation. A significant decrease in NFκB phosphorylation was seen in KPA-treated livers in the DIAMOND mouse model **(Figure 9K, Supplemental Fig 11N)**. In contrast, depletion of hepatic AMPK significantly augmented hepatic NFκB phosphorylation in KPA-treated mice **(Figure 9L,**

Supplemental Fig 11O). Together, these findings demonstrate an essential role for AMPK signaling downstream of KISS1R in regulating this process. HFD-fed LKO mice livers displayed increased hepatic NFκB phosphorylation, compared to controls (**Figure 9M**, **Supplemental Fig 11P).** Thus, these results suggest that one mechanism by which hepatic KISS1R signaling reverses advanced NASH is by suppressing hepatic NFκB signaling, downstream of AMPK activation. This thereby protects against HFD-induced liver steatosis and progression to NASH.

KISS1R signaling directly activates AMPK via $G\alpha_{q/11}$ and inhibits triglyceride synthesis in isolated primary mouse hepatocytes

Since our data revealed that KISS1R signaling inhibits steatosis in vivo, a direct effect of KP on hepatic lipogenesis was examined using isolated primary hepatocytes (56) which we observed express KISS1 in a punctate pattern typical of secreted peptides (**Figure 10A**). Next, hepatocytes isolated from *Kiss1r*$^{fl/fl}$ mice were cultured in the presence or absence of a mixture of FFAs (150 μM palmitate and 150 μM oleate conjugated to BSA (57) and treated with KISS1R agonists, kisspeptin-10 (KP10: 100 nM) or KPA (3 nM). Treatment of FFA loaded hepatocytes substantially decreased TG accumulation (**Figure 10B**). These KP concentrations were selected based on their ability to stimulate insulin secretion from isolated human pancreatic islets (58) and to activate KISS1R in vitro and in vivo (59-62). In contrast, KP failed to suppress TG levels in hepatocytes isolated from LKO mice (**Figure 10C**). KP treatment also reduced the expression of genes regulating DNL and TG synthesis in primary hepatocytes treated with FFAs (**Figure 10D**). KP stimulated phosphorylation of AMPK and its downstream target ACC, in control hepatocytes (**Figure 10E**, **Supplemental Figures 13A, B**). Phosphorylation of ACC at Ser-79 by AMPK reduces its activity, thereby inhibiting lipogenesis (63, 64). However, no change in

phosphorylation of AMPK or ACC was observed in hepatocytes isolated from LKO mice (**Figure 10E, Supplemental Figures 13A, B**). Kisspeptin induced AMPK phosphorylation was effectively blocked by selective AMPK inhibitor Compound C (**Figure 10F)** and also by the $G\alpha_{q/11}$-selective inhibitor, YM254890 (65-67) (**Figure 10G)** in isolated CTRL hepatocytes. Taken together, this suggests for the first time that kisspeptin signaling via KISS1R can directly activate AMPK in isolated primary hepatocytes.

KISS1R signaling increases fatty acid oxidation in isolated primary hepatocytes

AMPK increases mitochondrial CPT1 activity (68). The expression of CPT1α was downregulated in LKO mice (**Figure 2E**), indicating impaired β-oxidation, and increased upon KPA administration in livers from HFD-fed mice (**Figures 5B**). Thus, we investigated whether kisspeptin regulates fatty acid oxidation. Isolated primary mouse hepatocytes were treated with palmitate (100 μM) or BSA overnight and oxygen consumption rate (OCR) was measured using Seahorse XFe24 Analyzer (**Figures 11A-D**). KPA treatment in the presence of palmitate significantly enhanced basal OCR and ATP production compared to cells treated with palmitate alone (**Figures 11A, B, respectively**). KPA treatment also increased spare respiratory capacity, which indicates higher capability to generate ATP in response to metabolic stress. In contrast, KPA failed to increase OCR in hepatocytes isolated from LKO mice (**Figure 11A**). Similar observations were made using human hepatic HepaRG cells, where KPA treatment augmented OCR, in the presence of palmitate (**Supplementary Figure 13C-F**). To understand mechanistically the drastic differences in OCR between control and LKO hepatocytes, mitochondrial content was examined. This revealed a significant decrease in mitochondrial

markers voltage-dependent anion channel (VDAC), and cytochrome c oxidase I (COX1) in isolated hepatocytes LKO mice (**Figure 11 E; Supplementary Figure 13 G, H)**. The expression of VDAC and COX1 was also examined in livers from C57Bl/6J mice treated with KPA; there was a significant increase in the expression of both proteins in KPA-treated liver compared to controls (**Figure 11 F; Supplementary Figure 13I, J**). This finding implicates hepatic KISS1R signaling in regulating mitochondrial biogenesis. Taken together, findings suggest that enhanced activation of KISS1R negatively regulates hepatic lipid content by activating AMPK, which then inhibits lipogenesis and increases fatty acid oxidation. Hepatic AMPK activation downstream of KISS1R can also protect against inflammation by inhibiting NFκB signaling and alleviate hepatic fibrosis by decreasing fibrogenic signaling (**Figure 11G**).

KISS1/KISS1R expression and plasma KP are upregulated in human NAFLD/NASH patients

Since we found that HFD induced the expression of hepatic *Kiss1* and *Kiss1r* and increased plasma KP levels in mouse model of NAFLD (**Figures 1A, B**), we determined the clinical relevance of these findings in NAFLD. To that end, *KISS1* and *KISS1R* expression were examined in human liver biopsies from NAFL and NASH patients. There was a significant increase in *KISS1* and *KISS1R* mRNA and protein levels in human NAFL/NASH liver samples compared to healthy subjects (**Figures 12A, B; Supplemental Table 1**). Immunohistochemical analysis revealed enriched KISS1R expression localized to the plasma membrane and cytosol in human NAFL/NASH liver samples, compared to healthy liver (**Figure 12C**). Next, plasma KP levels were examined in male NAFL/NASH patients compared with healthy subjects, as previously described (69, 70). Since the prevalence of NAFLD parallels the rise of T2D, plasma KP levels were also examined in T2D patients. Plasma KP levels were measured among the following patient groups

(see **Table 1** for patient demographics): (1) healthy, (2) T2D, (3) fatty liver (NAFL), and (4) NASH. The data revealed that plasma KP levels were significantly higher in NAFL and NASH patients compared with the levels observed in T2D or healthy males (**Figure 12D**, mean ± S.E.M: healthy: 6.6± 0.8, T2D: 7.1 ± 0.7, NAFL:19.2 ± 2.6 and NASH: 18.9 ± 2.4 pmol/L). This indicates that the increased plasma KP levels are associated with liver injury. Overall, the data suggest that the KISS1/KISS1R signaling pathway is enhanced in patients with liver disease possibly as an adaptive mechanism in response to injury of the liver.

Discussion

In this report, we provide the first evidence of KISS1R as a key regulator of hepatic lipogenesis. Although KISS1 and KISS1R are expressed in the liver (9, 10), their biological function in the liver remained unknown. The goal of the present study was to determine the role of KISS1R in the development and progression of NAFLD. We found that HFD induced the expression of hepatic *Kiss1* and *Kiss1r* and increased plasma KPs in a mouse model of NAFLD. Using hepatic *Kiss1r* knockout (LKO) mice, we found that hepatic *Kiss1r* deficiency dramatically exacerbated hepatic steatosis compared to littermate controls on HFD. HFD-fed LKO mice showed aggravated metabolic parameters such as elevated levels of liver TGs, elevated fasting glucose and insulin resistance in addition to an increase in inflammatory and fibrosis markers. These phenotypes suggest that under pathophysiological conditions such as obesity and insulin resistance, hepatic KISS1R plays a crucial role in suppressing the development of the NAFLD phenotype by reducing hepatic lipogenesis.

Metabolic disease, like NAFLD, is well characterized by an alteration in glucose homeostasis, hyperinsulinemia and hypertriglyceridemia. Under conditions of selective insulin

505 resistance, insulin fails to suppress hepatic glucose production while augmenting hepatic
506 lipogenesis and TG accumulation(71). HFD-fed LKO mice display an increase in basal insulin
507 levels suggesting that hyperinsulinemia could contribute to the pathophysiology observed.

508 Despite the increase in plasma KP and hepatic *KISS1/KISS1R* levels observed in a mouse
509 model of NAFLD or in NAFLD patient livers, the endogenous activation of the KISS1R signaling
510 pathway is clearly not sufficient to safeguard against disease progression. Thus, to test the
511 hypothesis that enhanced activation of KISS1R signaling pathway plays a protective role in
512 NAFLD, we used two HFD-fed mouse models of NAFLD, which were treated with KPA, a potent,
513 protease-resistant KP analog (34). We found that KPA treatment in insulin resistant wild-type
514 C57BL/6J mice and DIAMOND mice reduced hepatic steatosis, decreased liver enzyme ALT and
515 reduced serum TGs, FFA and cholesterol. Mechanistically, it was observed that KPA treatment in
516 C57BL/6J mice decreased lipogenic regulators, although this was not consistently observed in
517 DIAMOND mice despite receiving the same duration of KPA treatment (5-6 weeks). This could
518 be due to the advanced NASH disease status of the DIAMOND mice that displayed F3 bridging
519 fibrosis (39 weeks on Western diet/sugar water), in contrast to early disease state (ie DNL)
520 observed in wild-type C57BL/6J mice (12 weeks on HFD), in addition to any differences in the
521 background strains of mice. Hepatic fibrosis, which predicts mortality and disease severity (72),
522 results from the activation of various pathways such as inflammation, oxidative stress (due to
523 mitochondrial dysfunction) and hepatic injury. As disease progresses, liver injury worsens fibrosis
524 without changes in hepatic steatosis (73). Notably, KPA administration reduced inflammatory and
525 fibrogenic signaling in both models, and demonstrated a therapeutic effect on liver fibrosis in the
526 DIAMOND mice.

Hepatic AMPK activity is considerably diminished in NAFL and NASH (73, 74), and this is linked to the incidence of NAFLD (75), whereas AMPK activation improves NAFL and NASH (74, 76). Our findings reveal that KISS1R activates AMPK in vivo in HFD livers, and directly in isolated hepatocytes, leading to an inhibition of TG accumulation. In stark contrast, KPA failed to protect against NAFLD in livers depleted of AMPK or KISS1R. These findings demonstrate a critical protective role of KP/KISS1R signaling in the development of NAFL and its progression to NASH and fibrosis, in an AMPK-dependent manner (**Fig. 11G**).

In chronic liver disease, hepatic stellate cells (HSCs) are direct mediators of fibrosis (5, 24). Growth factors such as TGFβ and inflammatory cytokines produced by other cell types such as macrophages cause HSCs to proliferate, transdifferentiate and become activated and secrete excessive amounts of extracellular matrix proteins that accumulate, leading to fibrosis and cirrhosis. AMPK activation has been shown to inhibit hepatic fibrosis by inhibiting HSC proliferation, by downregulating the expression of fibrogenic markers such as smooth muscle actin and TGFβ and decreasing oxidative stress (77). In addition, hepatic AMPK activation inhibits inflammation by attenuating po-inflammatory signaling, such as NFκB-mediated pathways (78). AMPK represses the nuclear localization of NFκB to thereby inhibit the expression of NFκB-target genes. Hepatic KISS1R activation by KPA inhibited nuclear NFκB phosphorylation in DIAMOND mice livers, and this repression was abolished upon depletion of hepatic KISS1R or hepatic AMPK. This demonstrates a vital role for hepatic AMPK in mediating the protective effects of KPA against NAFL and its progression to NASH and fibrosis.

Fatty acids are transported into the mitochondria for β-oxidation by CPT1. AMPK increases CPT1 activity and activates FAO by phosphorylation of ACC, to suppress its activity and thereby inhibit the production of malonyl-CoA, a potent allosteric inhibitor of CPT1 (63, 79).

While HFD-fed LKO mice displayed decreased *Cpt1a* expression and AMPK phosphorylation, KPA treatment in HFD-diet fed mice increased the expression of *Cpt1a* and AMPK activation and protected against NAFLD. Using isolated primary hepatocytes, we demonstrate KPA increases mitochondrial FAO which is repressed upon depletion of hepatic *Kiss1r*. This could be due to KISS1R signaling influencing hepatic mitochondrial biogenesis, although this requires further investigation. Interestingly, a recent study has demonstrated that KP10 administration promotes mitochondrial function in rat brain hippocampus via an AMPK-dependent pathway (80).

The link between KISS1 and mitochondrial function has been demonstrated in human melanoma cells by Welch and colleagues (81) whose pioneering work led to the initial discovery of *KISS1* as an anti-metastasis gene in melanoma cells (82). This study showed that overexpression of *KISS1* in human melanoma cells resulted in increased mitochondrial biogenesis and higher oxidation of fatty acids via β-oxidation, by inducing AMPK activation (81). These KISS1-mediated metabolic changes were essential for KISS1 to suppress melanoma cell invasion and metastasis (83). KISS1 functions as a metastasis suppressor gene in many cancers (84). However, KISS1R signaling in cancer appears to be context specific. Our earlier work has shown that in triple negative breast cancer (TNBC), KISS1R signaling promotes tumor growth and metastasis (70). When ERα is re-expressed in TNBC cells, KISS1R is downregulated demonstrating that ERα negatively regulates KISS1R expression in TNBC (85). In native TNBC cells lacking ERα, KISS1R signaling promotes epithelial-mesenchymal transition, MAPK activation and cancer growth and invasion (70, 86-88). The role of KISS1 in hepatocellular carcinoma (HCC) has not been clearly established, although *loss* of KISS1 in human HCC is associated with an upregulation of MMP-9, and increased cell invasion (89) suggesting that KISS1 may function as a metastasis suppressor in HCC.

573 Despite the prediction that chronic infusion of KPA would have resulted in the
574 desensitization of the protective response, our observations do not provide evidence of this. We
575 previously showed that in cells expressing KISS1R, exposure to kisspeptin triggers rapid KISS1R
576 desensitization and recycling. However, because of the rapid nature of these events, at any given
577 point in time, there is a KP-responsive population of receptors at the cell surface. As a result, while
578 the receptor undergoes desensitization, the cell remains responsive to KP and exhibits prolonged
579 signaling (60, 90-92).

580 Our human data showed a significant increase in KISS1 and KISS1R levels in liver
581 biopsies and elevated plasma KP levels from NASH patients compared to healthy subjects. In
582 contrast, no difference in KP levels was observed in T2D patients compared to healthy controls.
583 These results illustrate the translational relevance of our pre-clinical findings as they mirror the
584 results that we observed using HFD-fed mice. Changes in human plasma KP levels have been
585 reported in puberty (93) and pregnancy (94), as well as in various cancers (69, 70, 95). In fact, in
586 proof-of-concept studies, KP has been used to identify the cause of pubertal delay in children and
587 to treat infertility in adults (96-98). Similar to our observations, compensatory upregulation has
588 been reported for other pathways regulating hepatic lipid homeostasis (99). These include other
589 endocrine hormones such as fibroblast growth factor 21 and growth differentiating factor 15,
590 which are elevated in NAFLD and are currently being evaluated clinically. Thus, the upregulation
591 of hepatic KISS1/KISS1R and plasma KP in NAFL/NASH may serve as a compensatory response
592 aiming to slow down or resolve the progression of NAFLD. Our data suggest that clinical studies
593 aimed at treating NAFL/NASH with kisspeptin peptides are warranted. In conclusion, this study
594 revealed that hepatic KISS1R signaling system inhibits NAFLD via AMPK, uncovering KISS1R
595 as a new promising therapeutic target for the treatment of NAFLD.

Methods

See Supplement Data for all methodologies and Statistics.

Study Approval

All animal procedures were approved by Rutgers University according to guidelines by the Institutional Animal Care and Use Committee. Patient blood collection was approved by the Institutional Review Board at Rutgers University and by the West London Research Ethics Committee (12/LO/0507).

Author Contributions

All authors provided critical review of the manuscript and their approval; contributions for each listed below. Mice and metabolic studies, Western blot, qPCR, immunostaining: S.G. M.D., V.O. H.J.K; primary hepatocytes and FAO studies: S.G, M.D, V. B, K.K (supervised by J.Y.G, M.B). Human studies: S.G, S. R. M.D, clinicians, A.S, V.R, H.W., P.R.B, A.A., C.I., P.M. and W.S.D. Mice generated: *Kiss1r*$^{fl/fl}$ (S.R), *Kiss1r*$^{Alb\text{-}Cre}$ (A.V.B); G.L.G: study design, resources. A.V.B, F.E.W, M.B: conceptualization, study design, analysis, data interpretation and resources. M.B. supervised the study, wrote the manuscript with S.G.

Acknowledgements

We thank: Oanh Le-Hoang for technical help and Alvin Crespo-Bellido for assistance with schematic. Work was supported by funds to: M.B. (IFNH Seed, Busch Biomedical, TechAdvance, RCLR Small grant, SDG); A.V.B. (Busch Biomedical); S.G (NIH IMSD Scholarship), A.S (NIH KL2TR003018), W.S.D. (NIHR Research Professorship), A.A. (NIHR Clinician Scientist Award),

C.I. (Imperial College-Biomedical Research Centre IPPRF Fellowship (P79696), W.S.D., A.A. and C.I. (NIHR Imperial Biomedical Research Center). J.Y.G (NIH grant 5R01CA237347-02).

References

1. Machado MV, and Cortez-Pinto H. Non-alcoholic fatty liver disease: what the clinician needs to know. *World J Gastroenterol.* 2014;20(36):12956-80.
2. Younossi ZM, Koenig AB, Abdelatif D, Fazel Y, Henry L, and Wymer M. Global epidemiology of nonalcoholic fatty liver disease-Meta-analytic assessment of prevalence, incidence, and outcomes. *Hepatology.* 2016;64(1):73-84.
3. Vos MB, Abrams SH, Barlow SE, Caprio S, Daniels SR, Kohli R, et al. NASPGHAN Clinical Practice Guideline for the Diagnosis and Treatment of Nonalcoholic Fatty Liver Disease in Children: Recommendations from the Expert Committee on NAFLD (ECON) and the North American Society of Pediatric Gastroenterology, Hepatology and Nutrition (NASPGHAN). *J Pediatr Gastroenterol Nutr.* 2017;64(2):319-34.
4. Ballestri S, Nascimbeni F, Baldelli E, Marrazzo A, Romagnoli D, and Lonardo A. NAFLD as a Sexual Dimorphic Disease: Role of Gender and Reproductive Status in the Development and Progression of Nonalcoholic Fatty Liver Disease and Inherent Cardiovascular Risk. *Adv Ther.* 2017;34(6):1291-326.
5. Diehl AM, and Day C. Cause, Pathogenesis, and Treatment of Nonalcoholic Steatohepatitis. *N Engl J Med.* 2017;377(21):2063-72.
6. Shirazi F, Wang J, and Wong RJ. Nonalcoholic Steatohepatitis Becomes the Leading Indication for Liver Transplant Registrants Among US Adults Born Between 1945 and 1965. *J Clin Exp Hepatol.* 2020;10(1):30-6.
7. Bhattacharya M, and Babwah AV. Kisspeptin: beyond the brain. *Endocrinology.* 2015;156(4):1218-27.
8. Wolfe A, and Hussain MA. The Emerging Role(s) for Kisspeptin in Metabolism in Mammals. *Front Endocrinol (Lausanne).* 2018;9:184.
9. Song WJ, Mondal P, Wolfe A, Alonso LC, Stamateris R, Ong BW, et al. Glucagon regulates hepatic kisspeptin to impair insulin secretion. *Cell Metab.* 2014;19(4):667-81.
10. Shoji I, Hirose T, Mori N, Hiraishi K, Kato I, Shibasaki A, et al. Expression of kisspeptins and kisspeptin receptor in the kidney of chronic renal failure rats. *Peptides.* 2010;31(10):1920-5.
11. Chen D, Cao S, Chang B, Ma T, Gao H, Tong Y, et al. Increasing hypothalamic nucleobindin 2 levels and decreasing hypothalamic inflammation in obese male mice via diet and exercise alleviate obesity-associated hypogonadism. *Neuropeptides.* 2019;74:34-43.
12. Junker AE, Gluud L, Holst JJ, Knop FK, and Vilsboll T. Diabetic and nondiabetic patients with nonalcoholic fatty liver disease have an impaired incretin effect and fasting hyperglucagonaemia. *J Intern Med.* 2016;279(5):485-93.
13. Yu S, Matsusue K, Kashireddy P, Cao WQ, Yeldandi V, Yeldandi AV, et al. Adipocyte-specific gene expression and adipogenic steatosis in the mouse liver due to peroxisome proliferator-activated receptor gamma1 (PPARgamma1) overexpression. *J Biol Chem.* 2003;278(1):498-505.
14. Lee YK, Park JE, Lee M, and Hardwick JP. Hepatic lipid homeostasis by peroxisome proliferator-activated receptor gamma 2. *Liver Res.* 2018;2(4):209-15.

15. Vidal-Puig A, Jimenez-Linan M, Lowell BB, Hamann A, Hu E, Spiegelman B, et al. Regulation of PPAR gamma gene expression by nutrition and obesity in rodents. *J Clin Invest.* 1996;97(11):2553-61.
16. Hu E, Kim JB, Sarraf P, and Spiegelman BM. Inhibition of adipogenesis through MAP kinase-mediated phosphorylation of PPARgamma. *Science.* 1996;274(5295):2100-3.
17. Zhou G, Myers R, Li Y, Chen Y, Shen X, Fenyk-Melody J, et al. Role of AMP-activated protein kinase in mechanism of metformin action. *J Clin Invest.* 2001;108(8):1167-74.
18. Browning JD, and Horton JD. Molecular mediators of hepatic steatosis and liver injury. *J Clin Invest.* 2004;114(2):147-52.
19. Iena FM, Jul JB, Vegger JB, Lodberg A, Thomsen JS, Bruel A, et al. Sex-Specific Effect of High-Fat Diet on Glycerol Metabolism in Murine Adipose Tissue and Liver. *Front Endocrinol (Lausanne).* 2020;11:577650.
20. Jelen S, Wacker S, Aponte-Santamaria C, Skott M, Rojek A, Johanson U, et al. Aquaporin-9 protein is the primary route of hepatocyte glycerol uptake for glycerol gluconeogenesis in mice. *J Biol Chem.* 2011;286(52):44319-25.
21. Rodriguez A, Catalan V, Gomez-Ambrosi J, and Fruhbeck G. Aquaglyceroporins serve as metabolic gateways in adiposity and insulin resistance control. *Cell Cycle.* 2011;10(10):1548-56.
22. Puri P, Baillie RA, Wiest MM, Mirshahi F, Choudhury J, Cheung O, et al. A lipidomic analysis of nonalcoholic fatty liver disease. *Hepatology.* 2007;46(4):1081-90.
23. Paradies G, Paradies V, Ruggiero FM, and Petrosillo G. Cardiolipin and mitochondrial function in health and disease. *Antioxid Redox Signal.* 2014;20(12):1925-53.
24. Friedman SL, Neuschwander-Tetri BA, Rinella M, and Sanyal AJ. Mechanisms of NAFLD development and therapeutic strategies. *Nat Med.* 2018;24(7):908-22.
25. Lee YS, Li P, Huh JY, Hwang IJ, Lu M, Kim JI, et al. Inflammation is necessary for long-term but not short-term high-fat diet-induced insulin resistance. *Diabetes.* 2011;60(10):2474-83.
26. Schumacher JD, Kong B, Pan Y, Zhan L, Sun R, Aa J, et al. The effect of fibroblast growth factor 15 deficiency on the development of high fat diet induced non-alcoholic steatohepatitis. *Toxicol Appl Pharmacol.* 2017;330:1-8.
27. Chang CC, Wu CL, Su WW, Shih KL, Tarng DC, Chou CT, et al. Interferon gamma-induced protein 10 is associated with insulin resistance and incident diabetes in patients with nonalcoholic fatty liver disease. *Sci Rep.* 2015;5:10096.
28. Mirea AM, Tack CJ, Chavakis T, Joosten LAB, and Toonen EJM. IL-1 Family Cytokine Pathways Underlying NAFLD: Towards New Treatment Strategies. *Trends Mol Med.* 2018;24(5):458-71.
29. Syn WK, Choi SS, and Diehl AM. Apoptosis and cytokines in non-alcoholic steatohepatitis. *Clin Liver Dis.* 2009;13(4):565-80.
30. Delire B, Starkel P, and Leclercq I. Animal Models for Fibrotic Liver Diseases: What We Have, What We Need, and What Is under Development. *J Clin Transl Hepatol.* 2015;3(1):53-66.
31. Thompson EL, Murphy KG, Patterson M, Bewick GA, Stamp GW, Curtis AE, et al. Chronic subcutaneous administration of kisspeptin-54 causes testicular degeneration in adult male rats. *Am J Physiol Endocrinol Metab.* 2006;291(5):E1074-82.

32. Calder M, Chan YM, Raj R, Pampillo M, Elbert A, Noonan M, et al. Implantation failure in female Kiss1-/- mice is independent of their hypogonadic state and can be partially rescued by leukemia inhibitory factor. *Endocrinology.* 2014;155(8):3065-78.
33. Matsui H, Masaki T, Akinaga Y, Kiba A, Takatsu Y, Nakata D, et al. Pharmacologic profiles of investigational kisspeptin/metastin analogues, TAK-448 and TAK-683, in adult male rats in comparison to the GnRH analogue leuprolide. *Eur J Pharmacol.* 2014;735:77-85.
34. Asami T, Nishizawa N, Matsui H, Nishibori K, Ishibashi Y, Horikoshi Y, et al. Design, synthesis, and biological evaluation of novel investigational nonapeptide KISS1R agonists with testosterone-suppressive activity. *J Med Chem.* 2013;56(21):8298-307.
35. MacLean DB, Matsui H, Suri A, Neuwirth R, and Colombel M. Sustained exposure to the investigational Kisspeptin analog, TAK-448, down-regulates testosterone into the castration range in healthy males and in patients with prostate cancer: results from two phase 1 studies. *J Clin Endocrinol Metab.* 2014;99(8):E1445-53.
36. Ishikawa K, Tanaka A, Kogame A, Watanabe T, Tagawa Y, and Matsui H. Usefulness of pharmacokinetic/efficacy analysis of an investigational kisspeptin analog, TAK-448, in quantitatively evaluating anti-tumor growth effect in the rat VCaP androgen-sensitive prostate cancer model. *Eur J Pharmacol.* 2018;828:126-34.
37. Millar RP, and Babwah AV. KISS1R: Hallmarks of an Effective Regulator of the Neuroendocrine Axis. *Neuroendocrinology.* 2015;101(3):193-210.
38. Shao D, Rangwala SM, Bailey ST, Krakow SL, Reginato MJ, and Lazar MA. Interdomain communication regulating ligand binding by PPAR-gamma. *Nature.* 1998;396(6709):377-80.
39. Rochette-Egly C. Nuclear receptors: integration of multiple signalling pathways through phosphorylation. *Cell Signal.* 2003;15(4):355-66.
40. Szereszewski JM, Pampillo M, Ahow MR, Offermanns S, Bhattacharya M, and Babwah AV. GPR54 regulates ERK1/2 activity and hypothalamic gene expression in a Galpha(q/11) and beta-arrestin-dependent manner. *PLoS One.* 2010;5(9):e12964.
41. Sozio MS, Lu C, Zeng Y, Liangpunsakul S, and Crabb DW. Activated AMPK inhibits PPAR-{alpha} and PPAR-{gamma} transcriptional activity in hepatoma cells. *Am J Physiol Gastrointest Liver Physiol.* 2011;301(4):G739-47.
42. Leff T. AMP-activated protein kinase regulates gene expression by direct phosphorylation of nuclear proteins. *Biochem Soc Trans.* 2003;31(Pt 1):224-7.
43. Li Y, Xu S, Mihaylova MM, Zheng B, Hou X, Jiang B, et al. AMPK phosphorylates and inhibits SREBP activity to attenuate hepatic steatosis and atherosclerosis in diet-induced insulin-resistant mice. *Cell Metab.* 2011;13(4):376-88.
44. Quiroga AD, and Lehner R. Pharmacological intervention of liver triacylglycerol lipolysis: The good, the bad and the ugly. *Biochem Pharmacol.* 2018;155:233-41.
45. Kamari Y, Shaish A, Vax E, Shemesh S, Kandel-Kfir M, Arbel Y, et al. Lack of interleukin-1alpha or interleukin-1beta inhibits transformation of steatosis to steatohepatitis and liver fibrosis in hypercholesterolemic mice. *J Hepatol.* 2011;55(5):1086-94.
46. Foretz M, Ancellin N, Andreelli F, Saintillan Y, Grondin P, Kahn A, et al. Short-term overexpression of a constitutively active form of AMP-activated protein kinase in the liver leads to mild hypoglycemia and fatty liver. *Diabetes.* 2005;54(5):1331-9.

47. Asgharpour A, Cazanave SC, Pacana T, Seneshaw M, Vincent R, Banini BA, et al. A diet-induced animal model of non-alcoholic fatty liver disease and hepatocellular cancer. *J Hepatol.* 2016;65(3):579-88.
48. Chen CZ, and Raghunath M. Focus on collagen: in vitro systems to study fibrogenesis and antifibrosis state of the art. *Fibrogenesis Tissue Repair.* 2009;2:7.
49. Cissell DD, Link JM, Hu JC, and Athanasiou KA. A Modified Hydroxyproline Assay Based on Hydrochloric Acid in Ehrlich's Solution Accurately Measures Tissue Collagen Content. *Tissue Eng Part C Methods.* 2017;23(4):243-50.
50. Sluse FE, Jarmuszkiewicz W, Navet R, Douette P, Mathy G, and Sluse-Goffart CM. Mitochondrial UCPs: new insights into regulation and impact. *Biochim Biophys Acta.* 2006;1757(5-6):480-5.
51. Rippe C, Berger K, Boiers C, Ricquier D, and Erlanson-Albertsson C. Effect of high-fat diet, surrounding temperature, and enterostatin on uncoupling protein gene expression. *Am J Physiol Endocrinol Metab.* 2000;279(2):E293-300.
52. Caron A, Labbe SM, Carter S, Roy MC, Lecomte R, Ricquier D, et al. Loss of UCP2 impairs cold-induced non-shivering thermogenesis by promoting a shift toward glucose utilization in brown adipose tissue. *Biochimie.* 2017;134:118-26.
53. Sharma BK, Patil M, and Satyanarayana A. Negative regulators of brown adipose tissue (BAT)-mediated thermogenesis. *J Cell Physiol.* 2014;229(12):1901-7.
54. Foretz M, Even PC, and Viollet B. AMPK Activation Reduces Hepatic Lipid Content by Increasing Fat Oxidation In Vivo. *Int J Mol Sci.* 2018;19(9).
55. Zhang X, Liu S, Zhang C, Zhang S, Yue Y, Zhang Y, et al. The role of AMPKalpha2 in the HFD-induced nonalcoholic steatohepatitis. *Biochim Biophys Acta Mol Basis Dis.* 2020;1866(10):165854.
56. Kalemba KM, Wang Y, Xu H, Chiles E, McMillin SM, Kwon H, et al. Glycerol induces G6pc in primary mouse hepatocytes and is the preferred substrate for gluconeogenesis both in vitro and in vivo. *J Biol Chem.* 2019;294(48):18017-28.
57. Nagarajan SR, Paul-Heng M, Krycer JR, Fazakerley DJ, Sharland AF, and Hoy AJ. Lipid and glucose metabolism in hepatocyte cell lines and primary mouse hepatocytes: a comprehensive resource for in vitro studies of hepatic metabolism. *Am J Physiol Endocrinol Metab.* 2019;316(4):E578-E89.
58. Izzi-Engbeaya C, Comninos AN, Clarke SA, Jomard A, Yang L, Jones S, et al. The effects of kisspeptin on beta-cell function, serum metabolites and appetite in humans. *Diabetes Obes Metab.* 2018;20(12):2800-10.
59. Zhou Z, Lin Q, Xu X, Illahi GS, Dong C, and Wu X. Maternal high-fat diet impairs follicular development of offspring through intraovarian kisspeptin/GPR54 system. *Reprod Biol Endocrinol.* 2019;17(1):13.
60. Babwah AV, Pampillo M, Min L, Kaiser UB, and Bhattacharya M. Single-cell analyses reveal that KISS1R-expressing cells undergo sustained kisspeptin-induced signaling that is dependent upon an influx of extracellular Ca2+. *Endocrinology.* 2012;153(12):5875-87.
61. Liu H, Xu G, Yuan Z, Dong Y, Wang J, and Lu W. Effect of kisspeptin on the proliferation and apoptosis of bovine granulosa cells. *Anim Reprod Sci.* 2017;185:1-7.

62. Zajac M, Law J, Cvetkovic DD, Pampillo M, McColl L, Pape C, et al. GPR54 (KISS1R) transactivates EGFR to promote breast cancer cell invasiveness. *PLoS One.* 2011;6(6):e21599.
63. Munday MR, Campbell DG, Carling D, and Hardie DG. Identification by amino acid sequencing of three major regulatory phosphorylation sites on rat acetyl-CoA carboxylase. *Eur J Biochem.* 1988;175(2):331-8.
64. Ha J, Daniel S, Broyles SS, and Kim KH. Critical phosphorylation sites for acetyl-CoA carboxylase activity. *J Biol Chem.* 1994;269(35):22162-8.
65. Takasaki J, Saito T, Taniguchi M, Kawasaki T, Moritani Y, Hayashi K, et al. A novel Galphaq/11-selective inhibitor. *J Biol Chem.* 2004;279(46):47438-45.
66. Nishimura A, Kitano K, Takasaki J, Taniguchi M, Mizuno N, Tago K, et al. Structural basis for the specific inhibition of heterotrimeric Gq protein by a small molecule. *Proc Natl Acad Sci U S A.* 2010;107(31):13666-71.
67. Parobchak N, Rao S, Negron A, Schaefer J, Bhattacharya M, Radovick S, et al. Uterine Gpr83 mRNA is highly expressed during early pregnancy and GPR83 mediates the actions of PEN in endometrial and non-endometrial cells. *F&S Science.* 2020;1(1):67-77.
68. Ke R, Xu Q, Li C, Luo L, and Huang D. Mechanisms of AMPK in the maintenance of ATP balance during energy metabolism. *Cell Biol Int.* 2018;42(4):384-92.
69. Jayasena CN, Comninos AN, Januszewski A, Gabra H, Taylor A, Harvey RA, et al. Plasma kisspeptin: a potential biomarker of tumor metastasis in patients with ovarian carcinoma. *Clin Chem.* 2012;58(6):1061-3.
70. Dragan M, Nguyen MU, Guzman S, Goertzen C, Brackstone M, Dhillo WS, et al. G protein-coupled kisspeptin receptor induces metabolic reprograming and tumorigenesis in estrogen receptor-negative breast cancer. *Cell Death Dis.* 2020;11(2):106.
71. Brown MS, and Goldstein JL. Selective versus total insulin resistance: a pathogenic paradox. *Cell Metab.* 2008;7(2):95-6.
72. Hagstrom H, Nasr P, Ekstedt M, Hammar U, Stal P, Hultcrantz R, et al. Fibrosis stage but not NASH predicts mortality and time to development of severe liver disease in biopsy-proven NAFLD. *J Hepatol.* 2017;67(6):1265-73.
73. Zhao P, Sun X, Chaggan C, Liao Z, In Wong K, He F, et al. An AMPK-caspase-6 axis controls liver damage in nonalcoholic steatohepatitis. *Science.* 2020;367(6478):652-60.
74. Smith BK, Marcinko K, Desjardins EM, Lally JS, Ford RJ, and Steinberg GR. Treatment of nonalcoholic fatty liver disease: role of AMPK. *Am J Physiol Endocrinol Metab.* 2016;311(4):E730-E40.
75. Ruderman N, and Prentki M. AMP kinase and malonyl-CoA: targets for therapy of the metabolic syndrome. *Nat Rev Drug Discov.* 2004;3(4):340-51.
76. Garcia D, Hellberg K, Chaix A, Wallace M, Herzig S, Badur MG, et al. Genetic Liver-Specific AMPK Activation Protects against Diet-Induced Obesity and NAFLD. *Cell Rep.* 2019;26(1):192-208 e6.
77. Liang Z, Li T, Jiang S, Xu J, Di W, Yang Z, et al. AMPK: a novel target for treating hepatic fibrosis. *Oncotarget.* 2017;8(37):62780-92.
78. Luedde T, and Schwabe RF. NF-kappaB in the liver--linking injury, fibrosis and hepatocellular carcinoma. *Nat Rev Gastroenterol Hepatol.* 2011;8(2):108-18.

79. Jeon SM. Regulation and function of AMPK in physiology and diseases. *Exp Mol Med.* 2016;48(7):e245.
80. Mattam U, Talari NK, Paripati AK, Krishnamoorthy T, and Sepuri NBV. Kisspeptin preserves mitochondrial function by inducing mitophagy and autophagy in aging rat brain hippocampus and human neuronal cell line. *Biochim Biophys Acta Mol Cell Res.* 2021;1868(1):118852.
81. Manley SJ, Liu W, and Welch DR. The KISS1 metastasis suppressor appears to reverse the Warburg effect by shifting from glycolysis to mitochondrial beta-oxidation. *J Mol Med (Berl).* 2017;95(9):951-63.
82. Lee JH, Miele ME, Hicks DJ, Phillips KK, Trent JM, Weissman BE, et al. KiSS-1, a novel human malignant melanoma metastasis-suppressor gene. *J Natl Cancer Inst.* 1996;88(23):1731-7.
83. Liu W, Beck BH, Vaidya KS, Nash KT, Feeley KP, Ballinger SW, et al. Metastasis suppressor KISS1 seems to reverse the Warburg effect by enhancing mitochondrial biogenesis. *Cancer Res.* 2014;74(3):954-63.
84. Ly T, Harihar S, and Welch DR. KISS1 in metastatic cancer research and treatment: potential and paradoxes. *Cancer Metastasis Rev.* 2020;39(3):739-54.
85. Guzman S, Brackstone M, Wondisford F, Babwah AV, and Bhattacharya M. KISS1/KISS1R and Breast Cancer: Metastasis Promoter. *Semin Reprod Med.* 2019;37(4):197-206.
86. Blake A, Dragan M, Tirona RG, Hardy DB, Brackstone M, Tuck AB, et al. G protein-coupled KISS1 receptor is overexpressed in triple negative breast cancer and promotes drug resistance. *Sci Rep.* 2017;7:46525.
87. Cvetkovic D, Dragan M, Leith SJ, Mir ZM, Leong HS, Pampillo M, et al. KISS1R induces invasiveness of estrogen receptor-negative human mammary epithelial and breast cancer cells. *Endocrinology.* 2013;154(6):1999-2014.
88. Goertzen CG, Dragan M, Turley E, Babwah AV, and Bhattacharya M. KISS1R signaling promotes invadopodia formation in human breast cancer cell via beta-arrestin2/ERK. *Cell Signal.* 2016;28(3):165-76.
89. Shengbing Z, Feng LJ, Bin W, Lingyun G, and Aimin H. Expression of KiSS-1 gene and its role in invasion and metastasis of human hepatocellular carcinoma. *Anat Rec (Hoboken).* 2009;292(8):1128-34.
90. Pampillo M, and Babwah AV. Assessment of constitutive activity and internalization of GPR54 (KISS1-R). *Methods Enzymol.* 2010;484:75-93.
91. Pampillo M, and Babwah AV. Quantifying GPCR internalization: a focus on the Kisspeptin receptor. *Methods Mol Biol.* 2015;1272:119-32.
92. Min L, Soltis K, Reis AC, Xu S, Kuohung W, Jain M, et al. Dynamic kisspeptin receptor trafficking modulates kisspeptin-mediated calcium signaling. *Mol Endocrinol.* 2014;28(1):16-27.
93. Jayasena CN, Nijher GM, Narayanaswamy S, De Silva A, Abbara A, Ghatei MA, et al. Age-dependent elevations in plasma kisspeptin are observed in boys and girls when compared with adults. *Ann Clin Biochem.* 2014;51(Pt 1):89-96.
94. Romero-Ruiz A, Avendano MS, Dominguez F, Lozoya T, Molina-Abril H, Sangiao-Alvarellos S, et al. Deregulation of miR-324/KISS1/kisspeptin in early ectopic pregnancy:

mechanistic findings with clinical and diagnostic implications. *Am J Obstet Gynecol.* 2019;220(5):480 e1- e17.

95. Dhillo WS, Savage P, Murphy KG, Chaudhri OB, Patterson M, Nijher GM, et al. Plasma kisspeptin is raised in patients with gestational trophoblastic neoplasia and falls during treatment. *Am J Physiol Endocrinol Metab.* 2006;291(5):E878-84.

96. Chan YM, Lippincott MF, Kusa TO, and Seminara SB. Divergent responses to kisspeptin in children with delayed puberty. *JCI Insight.* 2018;3(8).

97. Millar RP, Sonigo C, Anderson RA, George J, Maione L, Brailly-Tabard S, et al. Hypothalamic-Pituitary-Ovarian Axis Reactivation by Kisspeptin-10 in Hyperprolactinemic Women With Chronic Amenorrhea. *J Endocr Soc.* 2017;1(11):1362-71.

98. George JT, Veldhuis JD, Tena-Sempere M, Millar RP, and Anderson RA. Exploring the pathophysiology of hypogonadism in men with type 2 diabetes: kisspeptin-10 stimulates serum testosterone and LH secretion in men with type 2 diabetes and mild biochemical hypogonadism. *Clin Endocrinol (Oxf).* 2013;79(1):100-4.

99. Ipsen DH, Lykkesfeldt J, and Tveden-Nyborg P. Molecular mechanisms of hepatic lipid accumulation in non-alcoholic fatty liver disease. *Cell Mol Life Sci.* 2018;75(18):3313-27.

GUZMAN ET AL FIGURE 1

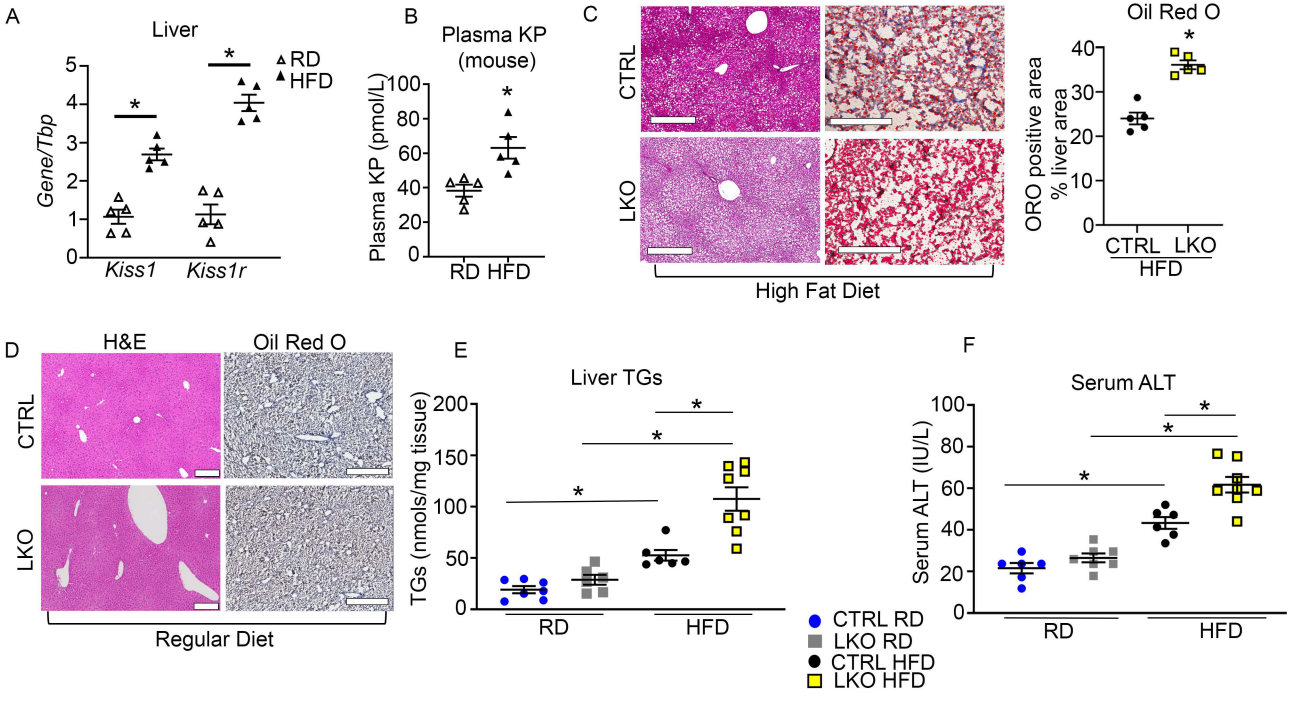

Figure 1. Hepatic *Kiss1r* knockout (LKO) mice exhibit increased hepatic steatosis in a diet induced mouse model of NAFLD. (A) Expression of Kiss1 and Kiss1r by RT-qPCR and (B) plasma KP levels in C57BL/6J male mice on regular diet (RD) or high fat diet (HFD) for 12 weeks. (C, D) Representative histology of liver sections for H&E (showing steatosis) or Oil Red O staining (showing lipids, red); quantification of staining shown in graph. Scale bars: 500 μm. No ORO staining observed in (D). (E) Liver triglycerides (TGs) and (F) serum alanine aminotransferase (ALT) levels in CTRL and LKO mice, 20 weeks on diet. Student's unpaired t-test or one-way ANOVA followed by Dunnett's post-doc test; *$p<0.05$ versus respective controls.

GUZMAN ET AL FIGURE 2

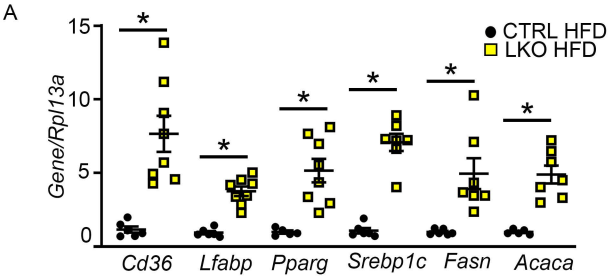

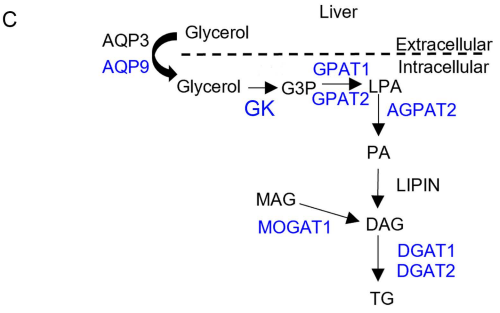

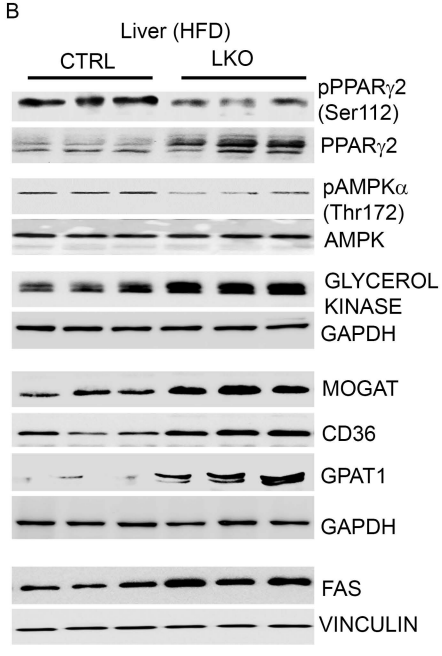

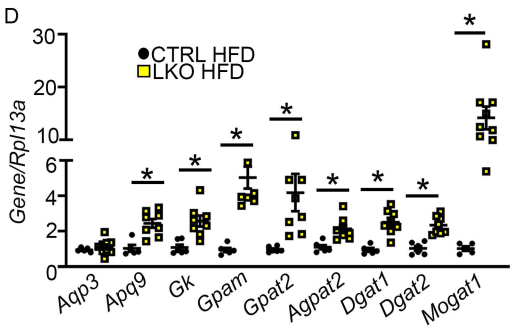

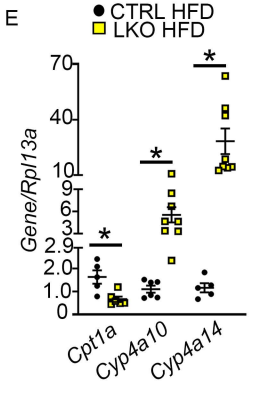

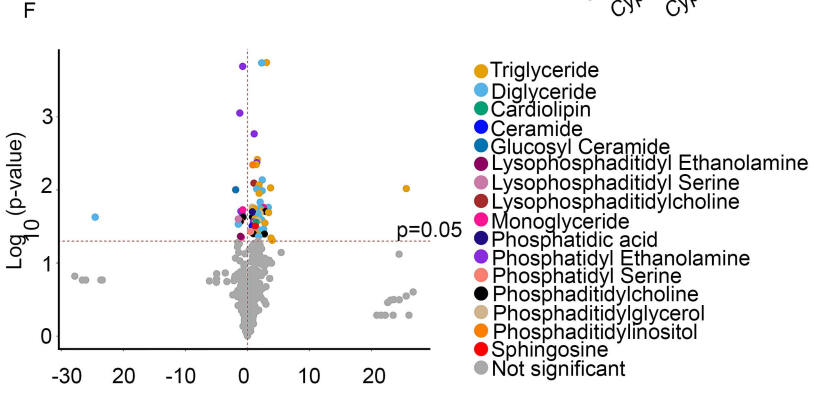

Figure 2. HFD fed- hepatic Kiss1r knockouts (LKO) exhibit increased expression of genes regulating triglyceride (TG) synthesis and enhanced liver lipid levels. (A) Expression of indicated genes by RT-qPCR. (B) Representative Western blots showing expression of indicated proteins. Densitometric analyses of blots and full blots are shown in Supplemental Figure 3. (C) Hepatic TG synthesis pathway; molecules upregulated in HFD LKO versus HFD CTRL livers (shown in blue). AQP, aquaporine; GK, glycerol kinase; G3P, glycerol-3-phosphate; LPA, lysophosphatidic acid; PA, phosphatidic acid, DAG, diacylglycerol; MAG, monoacylglycerol, TG, triglyceride. (D, E) Expression of indicated genes by RT-qPCR. (F) Volcano plot showing metabolites by LC-MS in HFD livers (CTRL vs. LKO). Mean +/- SEM shown. Student's unpaired t-test; *$p<0.05$ versus respective controls.

GUZMAN ET AL FIGURE 3

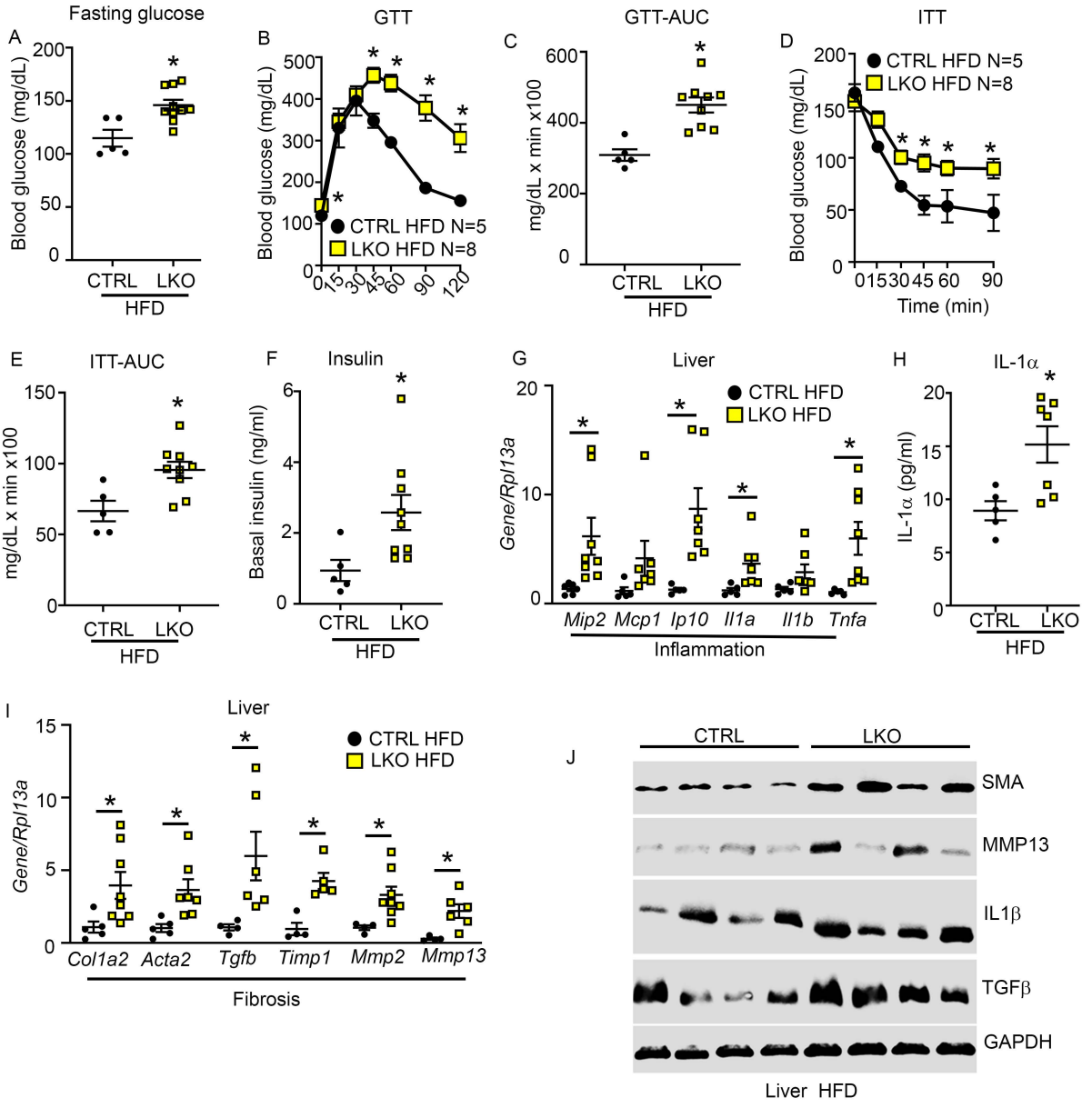

Figure 3. HFD fed-hepatic *Kiss1r* knockouts (LKO) mice are glucose intolerant and insulin resistant and exhibit increased inflammation and fibrosis markers. (A) Fasting blood glucose levels. Blood glucose levels during (B) a GTT and (C) area under the curve (AUC) of GTT; (D) an ITT and (E) AUC of ITT. (F) Basal insulin levels. (G) Expression of indicated genes by RT-qPCR. (H) Serum interleukin-1α levels. (I) Expression of indicated genes by RT-qPCR. (J) Expression of indicated protein by Western blot analysis. Densitometry analyses of blots shown in Supplemental Figure 3. Mean +/- SEM shown. Student's unpaired t-test or one-way ANOVA followed by Dunnett's post-hoc test; *$p<0.05$ versus respective controls.

GUZMAN ET AL FIGURE 4

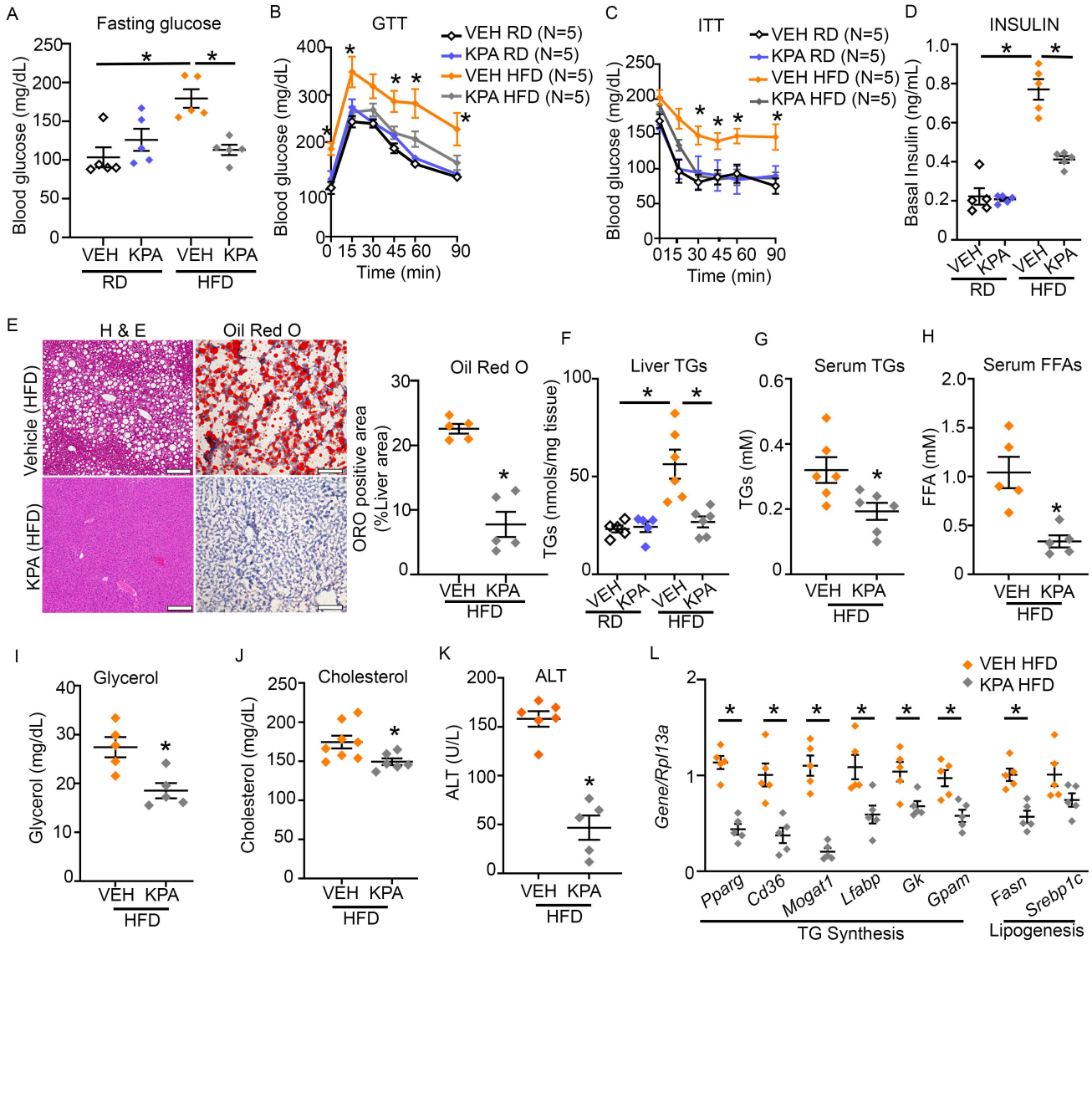

Figure 4. Kisspeptin-analog (KPA) treatment protects against insulin resistance and hepatic steatosis in HFD-fed mice. Blood glucose during (A) fasting (B) GTT (2.5 weeks on treatment) and in (C) ITT (3.5 weeks on treatment). (D) Basal insulin levels. (E) Representative histology of liver sections for H&E (left) and Oil red O (right) staining showing lipid accumulation (red); quantification of staining shown on the right. Scale bars: 200 μm. Endpoint (11 weeks on diet) measurements of (F) hepatic TG and serum (G) TGs, (H) FFA, (I) glycerol, (J) cholesterol and (K) ALT levels (5 weeks treatment). (L) Expression of indicated genes by RT-qPCR. Mean +/- SEM shown. Student's unpaired t-test or one-way ANOVA followed by Dunnett's post-hoc test. *$p<0.05$ versus respective controls.

GUZMAN ET AL FIGURE 5

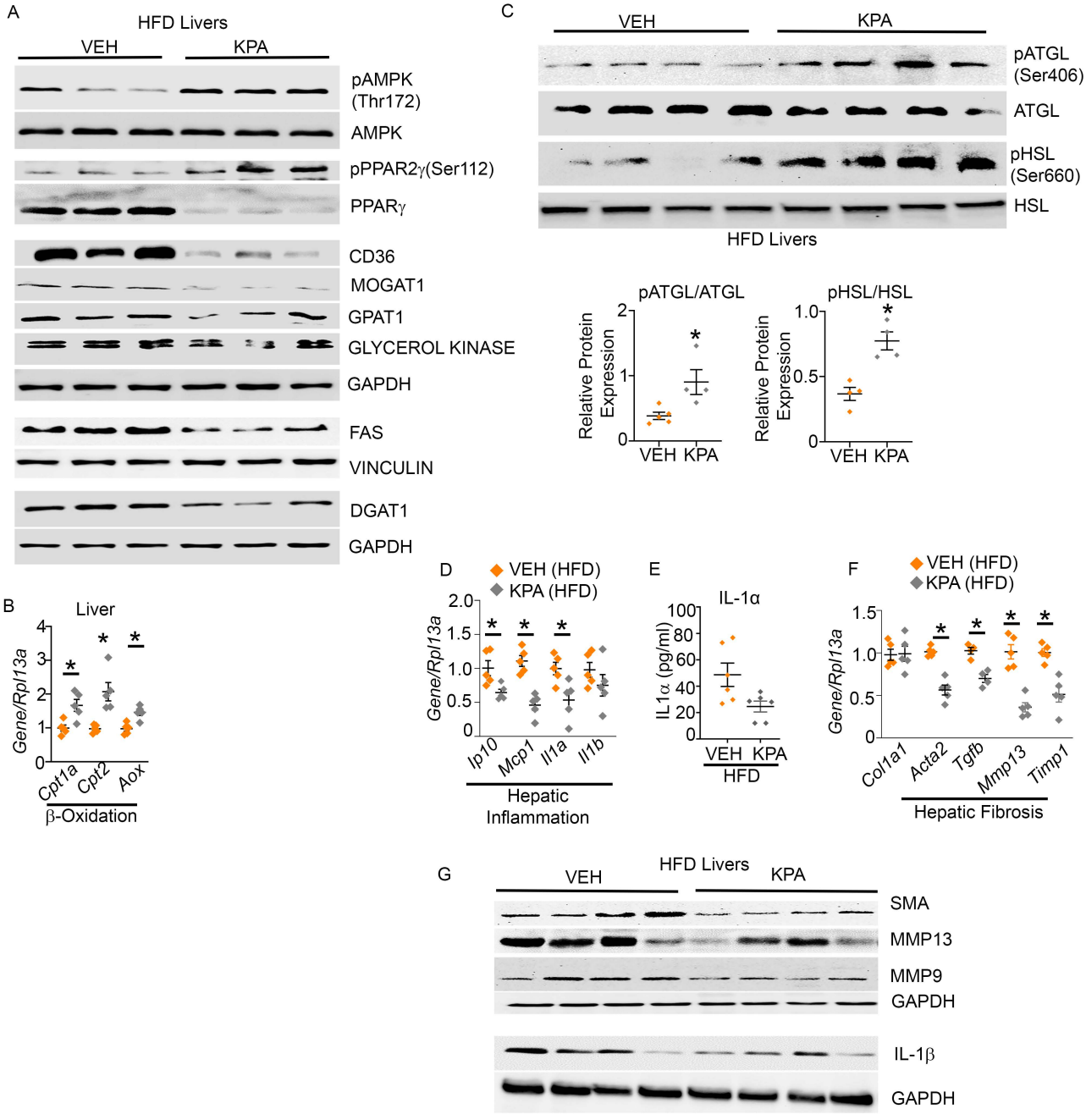

Figure 5. Kisspeptin-analog (KPA) treatment decreases markers of lipogenesis, inflammation and fibrosis in HFD-fed mice. (A) Representative Western blots showing expression of indicated proteins regulating lipogenesis. (B) Gene expression by RT-qPCR. (C) Representative Western blots showing indicated proteins and analyses of blots shown below. (D) Gene expression by RT-qPCR. (E) Serum interleukin 1α (IL1α) levels. (F) Gene expression by RT-qPCR. (G) Representative Western blots showing expression of indicated proteins. Densitometric analyses of blots in A and G and full blots shown in Supplemental Figure 5. Mean +/- SEM shown. Student's unpaired t-test; *$p<0.05$ versus respective controls.

GUZMAN ET AL FIGURE 6

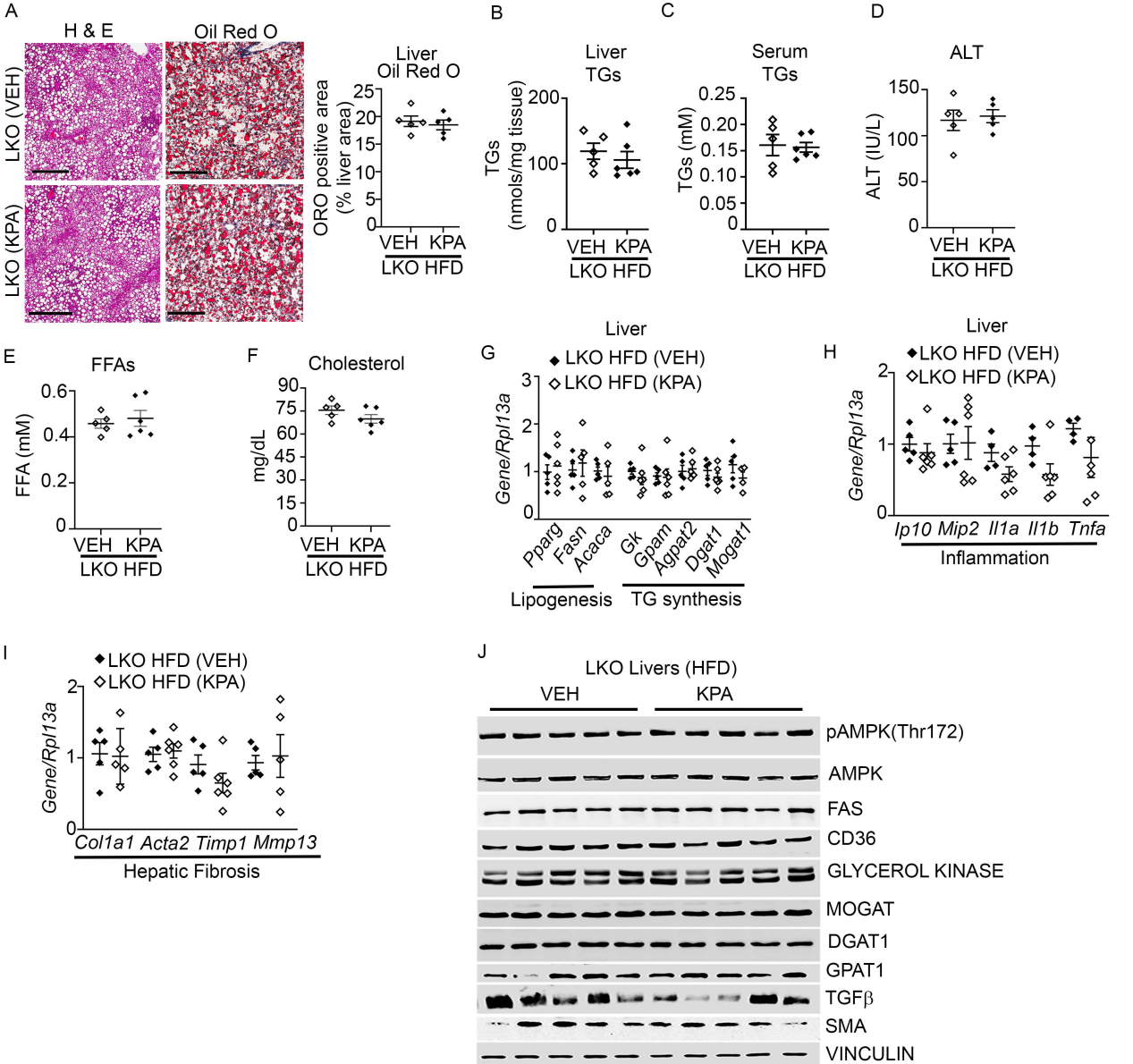

Figure 6. Lack of effect of kisspeptin-analog (KPA) treatment in hepatic *Kiss1r* knockout (LKO) mice on HFD. (A) Representative histology of liver sections for H&E showing steatosis (left) and Oil red O (right) staining showing lipid accumulation (red); quantification of staining (right). Scale bars: 200 μm. Levels of liver (B) and serum (C) triglyceride (TGs). Serum (D) ALT, (E) free fatty acids (FFA) and (F) cholesterol levels in LKO mice fed HFD for 11 weeks (G-I) Expression of indicated genes by RT-qPCR. (J) Representative Western blots showing expression of indicated proteins; densitometric analyses of blots shown in Supplemental Figure 8 (F-N). Mean +/- SEM shown. Student's unpaired t-test; *$p<0.05$ versus respective controls.

GUZMAN ET AL FIGURE 7

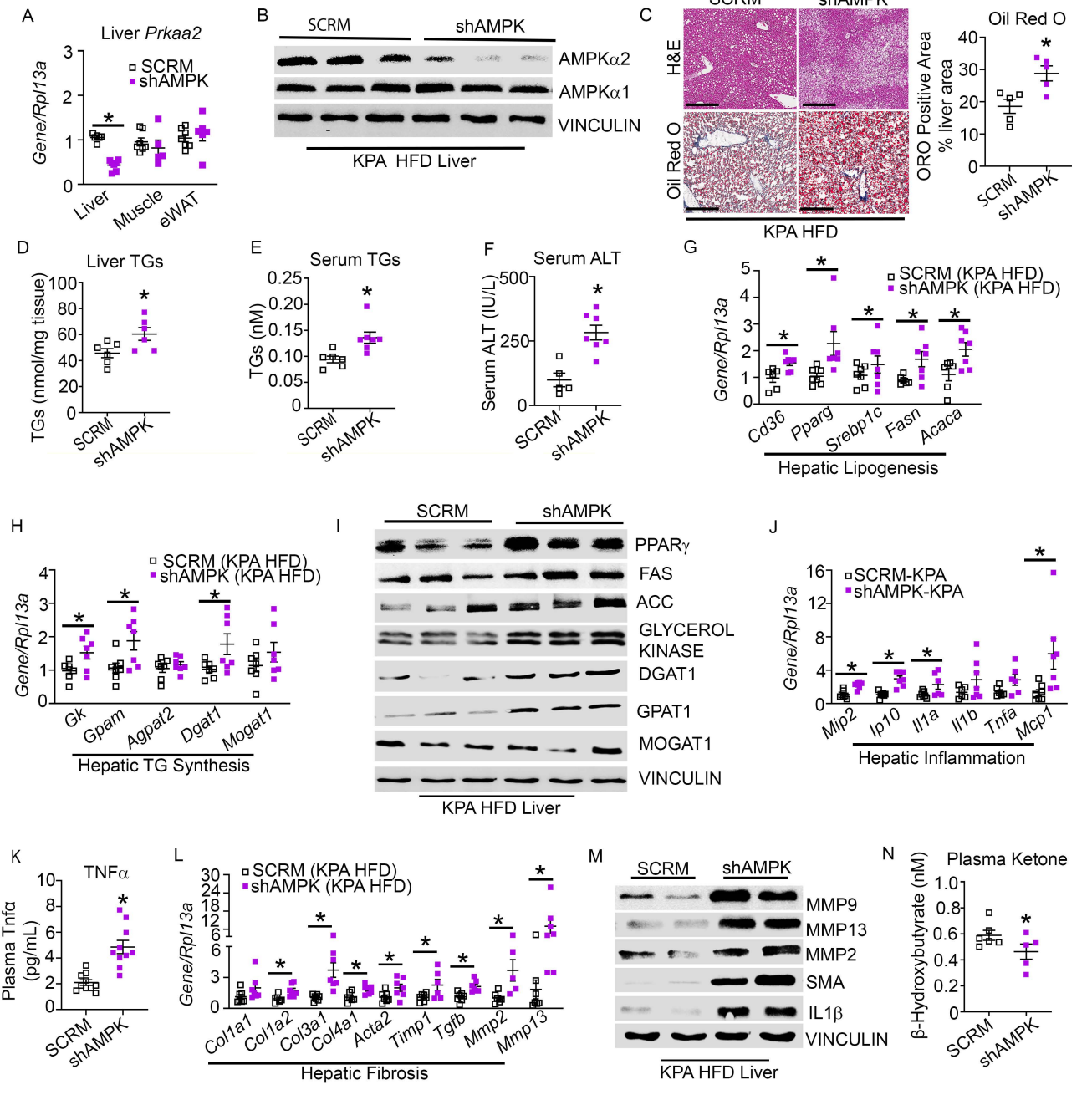

Figure 7. Lack of protective effect of KPA on steatosis and NASH progression in hepatic AMPK knockout mice on HFD. C57BL/6J mice on HFD were injected with either AAV8-U6-M-PRKAA2-shRNA (shAMPK) or AAV8-U6-M-SCRM-shRNA (SCRM) prior to KPA treatment, (A) Expression of *Prkaa2* (encodes AMPKα2) by RT-qPCR. (B) Representative Western blot showing expression of AMPK isoforms. (C) Representative histology of liver sections for H&E (left) and Oil red O (right) staining; quantification of staining shown on the right. Scale bar: 400 μm. Liver (D) and serum (E) TGs. (F) Serum ALT levels. (G, H, J, L) Expression of indicated genes by RT-qPCR. (I, M) Representative Western blots showing expression of indicated proteins. Plasma (K) TNFα levels and (N) ketone levels. Densitometric analyses of blots shown in Supplemental Figure 9 and full blots shown in Supplemental Figure 10. Mean +/- SEM shown. Student's unpaired t-test *$p<0.05$ versus respective controls.

GUZMAN ET AL FIGURE 8

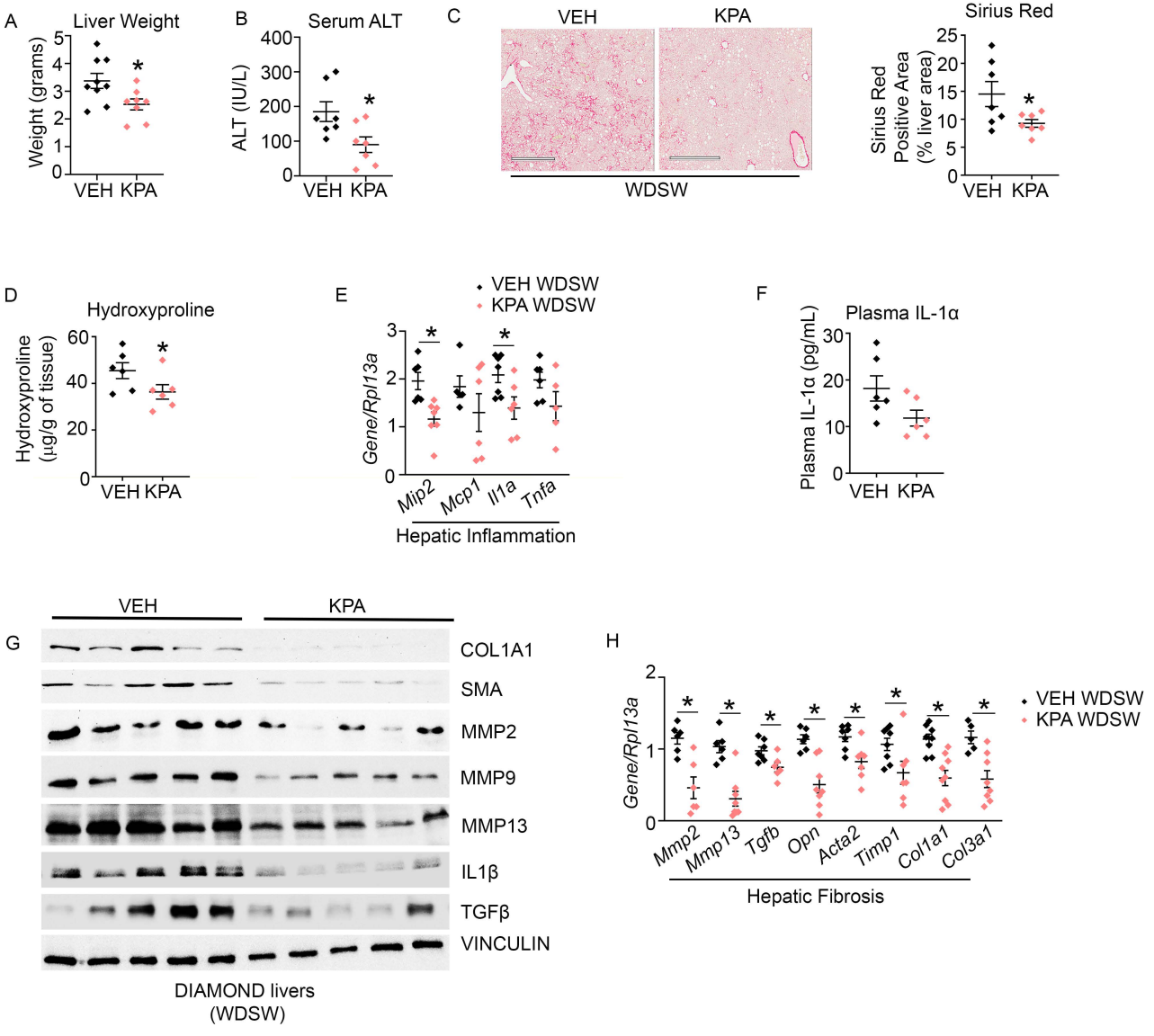

Figure 8. KPA treatment alleviates NASH in a Diet Induced Animal Model of Non-Alcoholic Liver Disease (DIAMOND) mice. DIAMOND mice maintained on a Western diet with sugar water (WDSW) for 33 weeks were treated with Vehicle (PBS) or KPA for 6 wks while kept on WDSW diet. (A) Liver weight at endpoint. (B) Serum ALT levels. (C) Representative histology of liver section showing picrosirius Red staining. Scale bar: 500 μm, graph: quantification of staining. (D) Liver hydroxyproline levels. (E) Expression of indicated hepatic genes by RT-qPCR. (F) Plasma IL-1α levels. (G) Representative Western blots showing expression of indicated proteins. (H) Expression of indicated hepatic genes by RT-qPCR. Densitometric analyses of blots shown in Supplemental Figure 10A-G. Mean +/- SEM shown. Student's unpaired t-test *$p<0.05$ versus respective controls.

GUZMAN ET AL FIGURE 9

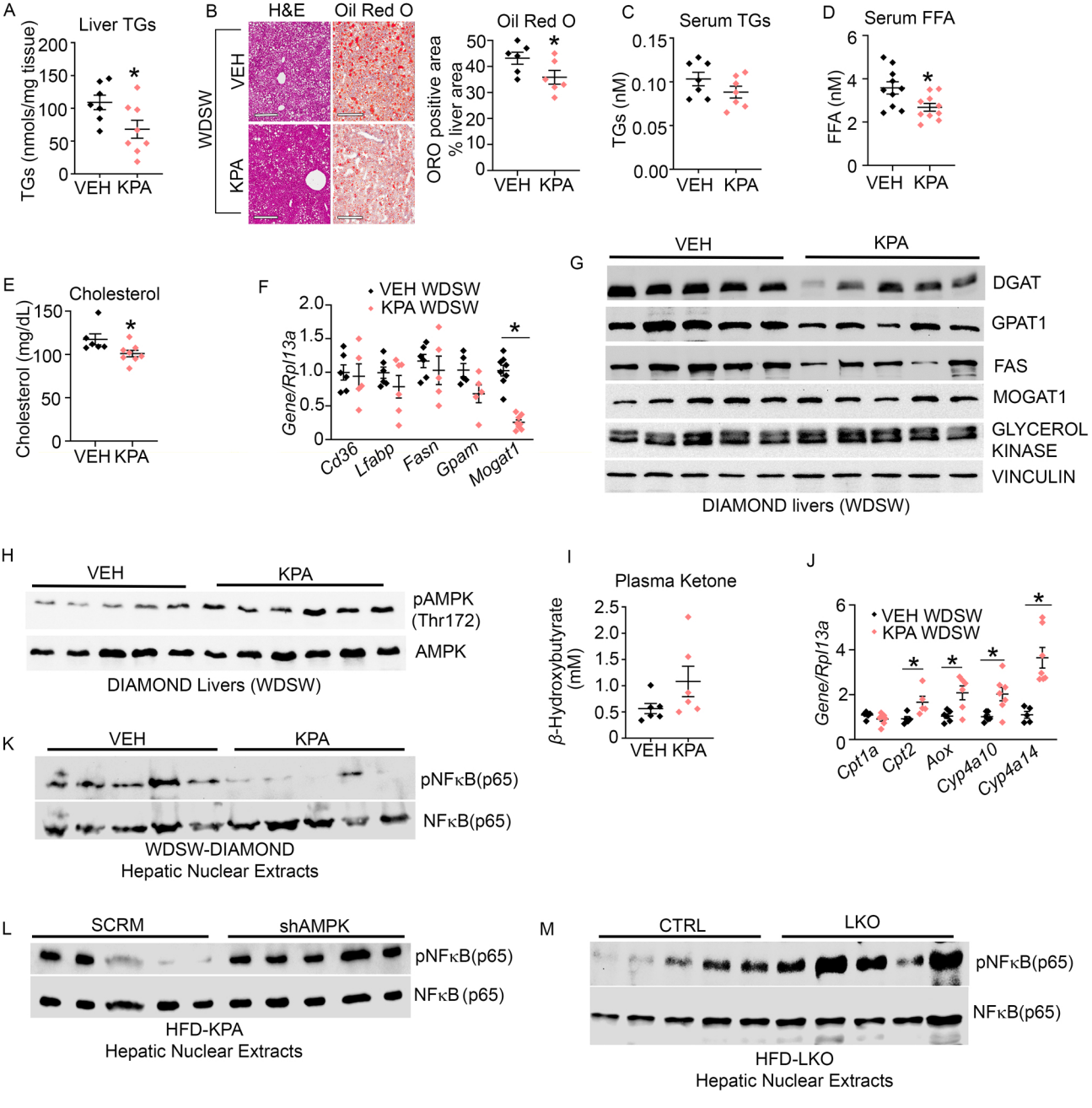

Figure 9. KISS1R agonist (KPA) alleviates NASH in DIAMOND mice fed WDSW.

DIAMOND mice on WDSW for 33 weeks were treated with VEH (PBS) or KPA for 6 weeks. (A) Liver TGs. (B) Representative liver histology for H&E and Oil Red O staining; quantification of staining shown on the right. Scale bar 500 μm. Serum (C) TGs levels. (D) Free Fatty Acid (FFA) levels and (E) cholesterol levels. (F) Expression of indicated genes by RT-qPCR. (G, H) Representative Western blot showing expression of indicated proteins. (I) β-Hydroxybutyrate levels. (J) Expression of indicated hepatic genes by RT-qPCR. Representative Western blot showing expression of indicated nuclear proteins in (K) DIAMOND mice livers (L) livers depleted of AMPK and (M) LKO HFD livers. Densitometric analyses of blots shown in Supplemental Figure 10N-P. Mean +/- SEM shown. Student's unpaired t-test *$p<0.05$ versus respective controls.

GUZMAN ET AL FIGURE 10

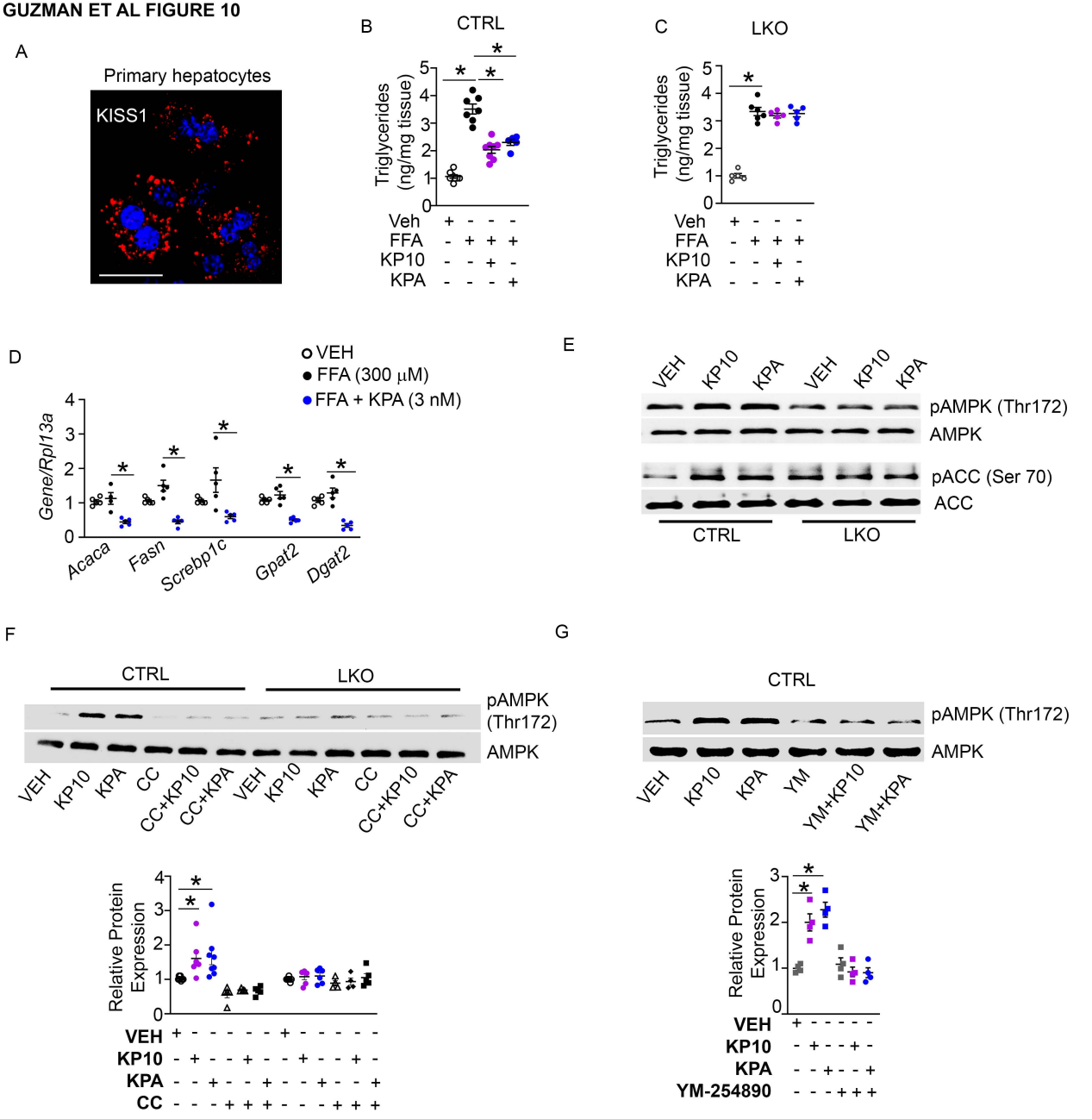

Figure 10. Kisspeptin inhibits TG accumulation in isolated primary mouse hepatocytes. (A) Representative confocal image of endogenous KISS1 immunostaining in Control (CTRL) hepatocytes. Scale bar, 50 μm. Effect of KP10 (100 nM) or KPA (3 nM) on TG accumulation (expressed as fold change over VEH) in (B) CTRL and (C) LKO hepatocytes treated with oleic and palmitic acid (150 μM each). (D) Expression of indicated genes by RT-qPCR. (E) Representative Western blots of indicated proteins in hepatocytes following KP10 (100 nM) or KPA (3 nM) treatment; quantification of blots in Supplemental Figure 12 A, B. Representative Western blots of indicated proteins in hepatocytes in the presence or absence of (F) Compound C (CC: 10 μM) treatment and quantification of blots and (G) YM-25489 (YM: 3μM) and quantification of blots. * $p < 0.05$ vs controls; One-way ANOVA followed by Dunnet's post-hoc test.

GUZMAN ET AL FIGURE 11

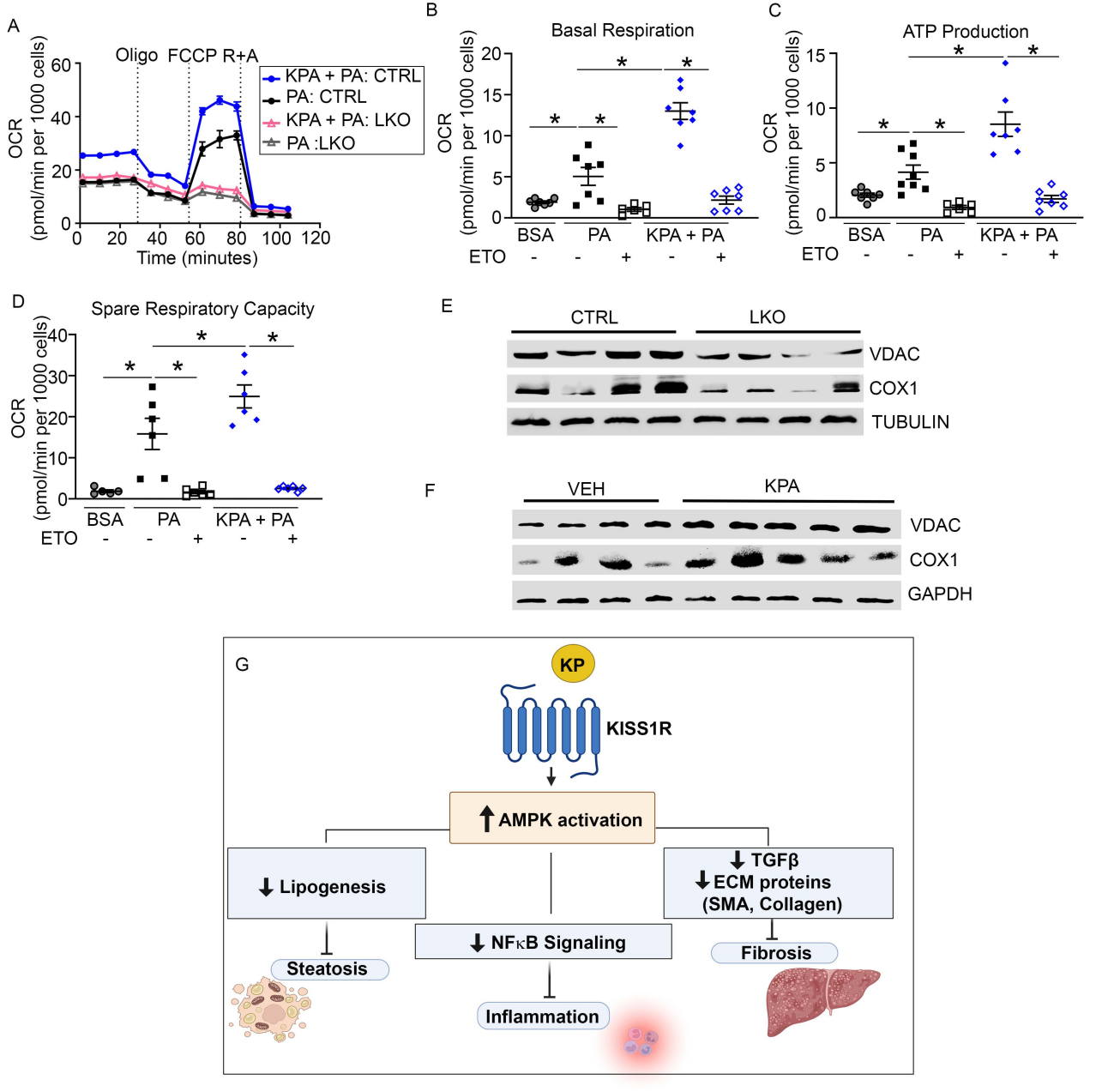

Figure 11. Kisspeptin increases Fatty Acid Oxidation in isolated primary mouse hepatocytes. (A-D) Oxygen consumption rate (OCR) in hepatocytes treated with 100 μM palmitate (PA) or BSA with or without KPA (3 nM) or CPT1 inhibitor, Etomoxir (ETO). Representative OCR trace using Seahorse analyzer shown in (A) following sequential treatment with 2.5 μM oligomycin (Oligo), 3 μM carbonyl cyanide-4 (trifluoromethoxy) phenylhydrazone (FCCP), an uncoupler of mitochondrial oxidative phosphorylation and 2.5 μM of Rotenone and antimycin A (R +A), complex I and III inhibitors. (E) Representative Western blot showing expression of indicated protein in primary hepatocytes isolated from CTRL and LKO livers; quantification in supplemental Figure 12G, H. (F) Representative Western blot showing expression of indicated protein in KPA treated HFD-fed mouse livers; quantification in supplemental Figure 12I, J. (G) Schematic showing proposed signaling pathways by which KISS1R activation suppresses hepatic lipogenesis and NASH progression.* $p < 0.05$ vs controls; One-way ANOVA followed by Dunnet's post-hoc test.

GUZMAN ET AL FIGURE 12

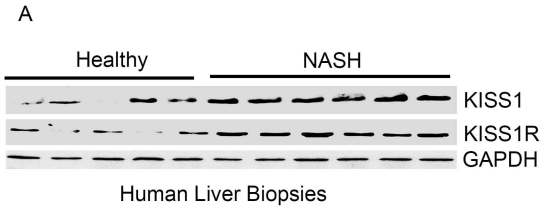

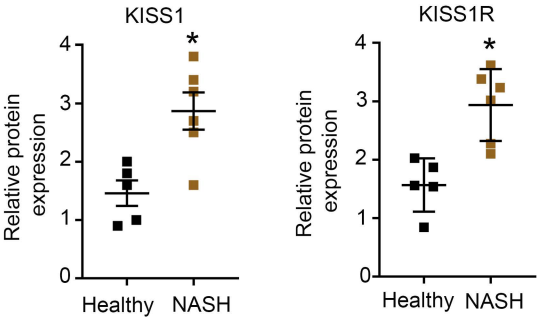

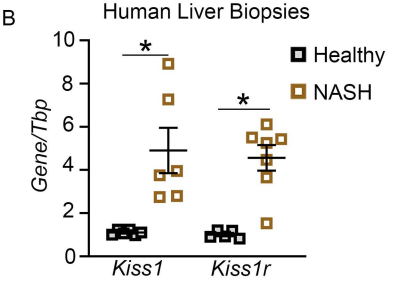

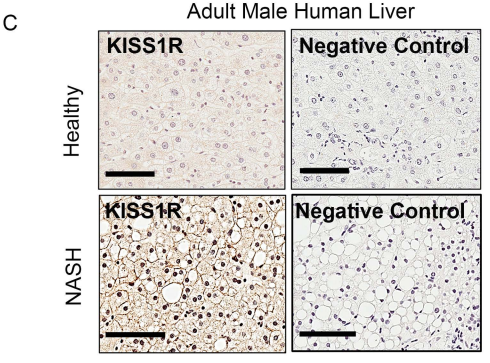

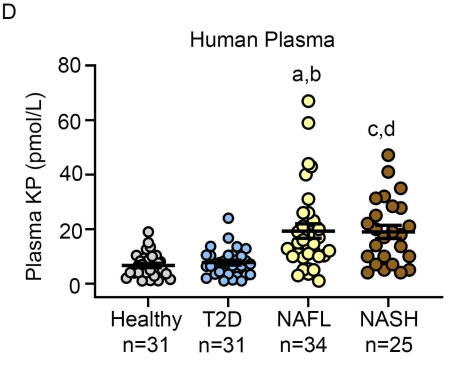

Figure 12. Hepatic KISS1/KISS1R expression and plasma kisspeptin levels are increased in male patients with NAFLD. (A) Representative Western blots and densitometric analysis of blots (right). (B) Expression of human *KISS1* and *KISS1R* by RT-qPCR. Mean +/- SEM shown, Student's unpaired t-test, *$p<0.05$ compared to controls. (C) Representative images showing immunostaining of endogenous KISS1R in liver; scale bar (80 μM). (D) Plasma kisspeptin (KP) levels (pmol/L; mean +/- S.E.M) in human subjects. Statistical analysis done using a non-parametric Kruskal-Wallis test. Error bars: S.E.M. T2D: type 2 diabetes; NAFL: non-alcoholic fatty liver disease; NASH: non-alcoholic steatohepatitis. a, $p<0.001$ for NAFL compared to healthy; b, $p<0.001$ for NAFL compared to T2D; c, $p<0.001$ for NASH compared to healthy and d, $p<0.001$ for NASH compared to T2D.

Table 1 Clinical profile of study participants from RWJMS, New Brunswick, NEW Jersey, U.S.A and Imperial College London/Imperial College Healthcare NHS Trust, U.K.

Reference ranges provided in blue below name of listed characteristic.

Variable (Reference Range)	Healthy n=31	T2D n=31	NAFL n=34	NASH n=25
Age (years)	30.97 ± 6.1 [d,f,s]	60.66 ± 11.62 [h]	50.82 ± 13.69 [h]	53.95 ± 11.32 [h]
Weight (kg)	73.22 ± 10.66 [d,f,s]	94.82 ± 18.85 [h]	99.89 ± 20.82 [h]	101.3 ± 28.42 [h]
BMI (kg/m^2) **18.5-24.9**	23.03 ± 3.97 [d,f,s]	30.95 ± 6.16 [h]	32.41 ± 5.16 [h]	33.99 ± 8.42 [h]
HbA1c (%) **< 5.7%**		8.27 ± 1.88 [f,s]	7.18 ± 1.45 [s]	5.83 ± 1.08
Glucose (mg/dL) **60-140mg/dL**		152.2 ± 60.20 [f]	124.7 ± 37.08 [d]	120.5 ± 56.42
Number of DM Medications		2.87 ± 1.36 [f,s]	1.88 ± 1.60 [d]	1.11 ± 0.88 [d]
Triglycerides (mg/dL) **0-149 mg/dL**		140.80 ± 62.94	175.0 ± 69.70	144.0 ± 86.96
HDL (mg/dL) **>39mg/dL**		39.85 ± 7.53	41.41 ± 10.31	48.49 ± 23.39
LDL (mg/dL) **0-99 mg/dL**		75.56 ± 27.54 [f]	104.0 ± 48.76 [d]	95.77 ± 33.17
AST (units/L) **0-40 units/L**		21.04 ± 7.48 [f,s]	38.45 ± 15.87 [d]	52.20 ± 29.66 [d]
ALT (units/L) **0-44 units/L**		23.00 ± 6.92 [f,s]	65.82 ± 41.66 [d]	66.75 ± 48.96 [d]
Total Bilirubin (mg/dL) **0-1.2 mg/dL**		0.50 ± 0.35 [s]	0.54 ± 0.23	1.28 ± 1.98 [d]
Albumin (g/dL) **3.5-4.8 g/dL**		4.23 ± 0.37 [f]	4.50 ± 0.33 [d,s]	4.16 ± 0.42 [f]
Platelets (x1000/uL) **150,000-450,000/uL**		213.50 ± 43.59	229.50 ± 82.02	188.8 ± 88.27
Creatinine (mg/dL) **0.76-1.27 mg/dL**		1.12 ± 0.48 [s]	0.96 ± 0.24	0.82 ± 0.21 [d]
Fib-4 Score **<1.45**			1.37 ± 1.34 [s]	2.67 ± 2.12 [f]

h: p<0.05 significance compared to healthy men
d: p<0.05 significance compared to men with T2D without NAFL/NASH
f: p<0.05 significance compared to men with NAFL
s: p<0.05 significance compared to men with NASH